Fall 1988

Glass formation and properties in the $Sm_2O_3 \cdot Al_2O_3 \cdot SiO_2$ system

Erik M. Erbe

GLASS FORMATION AND PROPERTIES IN THE $Sm_2O_3 \cdot Al_2O_3 \cdot SiO_2$ SYSTEM

BY

ERIK MICHAEL ERBE, 1965 -

A THESIS

Presented to the Faculty of the Graduate School of the

UNIVERSITY OF MISSOURI-ROLLA

In Partial Fulfillment of the Requirements for the Degree

MASTER OF SCIENCE IN CERAMIC ENGINEERING

1988

Approved by

Delbert E. Day (Advisor) Robert E. Moore

Leon F. Brown

PUBLICATION THESIS OPTION

This thesis has been prepared in the style utilized by the Journal of the American Ceramic Society. Pages 1 through 59 will be presented for publication in that journal. Appendices A, B, and C have been added for purposes normal to thesis writing.

ABSTRACT

The purpose of this investigation was to develop a samarium containing aluminosilicate glass with properties suitable for use in the treatment of rheumatoid arthritis. Microspheres made from these compositions would be neutron activated to produce radioactive Sm-153 which has beta-particle energies suitable for treating rheumatoid arthritis as well as appropriate gamma-ray emission for nuclear imaging. The properties of $Sm_2O_3 \cdot Al_2O_3 \cdot SiO_2$ glasses containing 10 to 25 mole% Sm_2O_3 were evaluated as a function of composition. The density, refractive index, thermal expansion coefficient, and microhardness increased with increasing Sm_2O_3 content. The dissolution rate in 1N HCl and deionized water at 37°C increased whereas the dissolution rate in deionized water at 70°C decreased with increasing Sm_2O_3 content. Several glasses had excellent properties suitable for radiotherapeutic applications. The composition range for the glasses best suited for these applications was (10-25) $Sm_2O_3 \cdot$ (20-35) $Al_2O_3 \cdot$ (40-70) SiO_2 (mole%).

ACKNOWLEDGEMENT

The author wishes to express his gratitude to Dr. D. E. Day at the Graduate Center for Materials Research, University of Missouri-Rolla for his guidance and encouragement throughout this project. Expressed thanks is also due to Dr. C. S. Ray, Dr. E. Lorey, and Dr. G. J. Ehrhardt for their helpful contributions. Special thanks is due my wife, Shannon, and daughter, Ashley, for their love, support, and patience.

This research was funded by a Weldon Springs Research Grant.

TABLE OF CONTENTS

LIST OF ILLUSTRATIONS

LIST OF TABLES

I. INTRODUCTION

Rheumatoid arthritis is a painful disease that afflicts the joints of millions of people. This disease is manifested in the synovial fluid and synovial membrane causing swollen joints, chronic inflammation, scarring of joints and excruciating pain.[1] Conventional methods of treating rheumatoid arthritis consist of the surgical removal of the diseased synovial tissue or externally irradiating the entire region at the diseased joint.[2] Surgical synovectomy is costly and painful. Furthermore, it is limited to a number of specific joints. External irradiation of the diseased tissue is somewhat successful, but is limited by the amount of radiation that can be administered without harming nearby, healthy tissue.[3] Irradiation of the diseased synovial tissue shows promise in slowing down the growth of diseased tissue. [4-6]

Injection of a radioactive material into the synovial sac of a joint is a feasible method of delivering a therapeutic dose of localized radiation to the diseased synovial tissue, while minimizing the harmful effects of the radiation on surrounding healthy tissue.[7,8] The radioactive material must not dissolve in the chemical environment of the body. Chemical dissolution of the radioactive material inside the body or its leakage from the joint can lead to the irradiation of healthy organs.[9] Previously used ^{90}Y Theraspheres™, an extremely durable yttria containing aluminosilicate glass, has proven effective in the treatment of liver cancer.[8] A chemically durable, neutron activatable glass has the advantage over conventional treatment methods in that it can deliver greater doses of radiation locally, with no leakage and minimum irradiation of healthy tissue. The success of

activatable glasses in the delivery of radiation to the liver has been the impetus for further studies of other similar activatable glass systems.

One of the primary characteristics of a neutron activatable glass for radiotherapeutic applications is high chemical durability. As shown by the ^{90}Y Theraspheres™, an aluminosilicate glass can provide the required chemical durability. Silicate glasses, in general, are excellent solvents for many cations, or in this application, elements which can be easily activated to a radionuclide. Because of its good chemical durability, an aluminosilicate glass can withstand in vivo conditions well past the lifetime of the radionuclide.[10,11] The wide compositional range for glass formation in silicate systems also enables the utilization of several isotopes with different radiation characteristics. Table I lists several elements having acceptable nuclear properties for use in radiotherapeutic microspheres.[12,13]

A second consideration for a neutron activatable glass is the radiation characteristics of the radionuclide. The required characteristics depend on the exact application and the region in the body where radiation is needed. In the treatment of diseased human tissue, beta-emitting radionuclides are preferred due to their low to moderate linear energy transfer distance (LET) of ionized particles and easy, copious production by neutron capture in a nuclear reactor.[11] The half life of a radionuclide is also a factor in selecting a radionuclide for a specific application. It is imperative that only the desired element be activated, so other constituents in the glass should have either negligible radiation emission energies or very short half lifes. Alumina and silica have negligible radiation emission energies after neutron activation.[14] All constituents in the glass should be biocompatible.

TABLE I

ELEMENTS HAVING ACCEPTABLE NUCLEAR PROPERTIES
FOR USE IN RADIOTHERAPEUTIC MICROSPHERES

-																-	-
Li	-											-	C	N	O	F	-
Na	Mg											Al	Si	P	-	-	-
K	-	-	Ti*	V	-	Mn	-	-	-	Cu*	-	Ga	Ge*	-	-	-	-
-	-	Y	Zr*	Nb	-	-	-	-	-	-	-	-	-	-	-	I	-
-	-	-	-	-	-	-	-	-	-	-	-	-	Pb	-	-	-	-

-	-	-	-	Sm	-	-	-	Dy	Ho	-	-	-	-		

* marginally acceptable nuclear properties

In vivo applications require that the materials be nontoxic and safely cleared from the body.[15]

Finally, the density of the glass used to make microspheres is important from an administration and production standpoint. The density of the glass is crucial to keeping the glass microspheres in suspension prior to injection into the body. This assures that the proper dosage is given. Glass microspheres can be kept in suspension by decreasing the density of the glass, decreasing the diameter of the microsphere, or by increasing the viscosity of the suspension liquid. One can accurately calculate the settling velocity, V, of a spherical particle in a liquid medium from Stoke's Law[16]

$$V = \frac{(\rho_g - \rho_l)\, g\, D^2}{18\eta} \qquad \text{.....} \qquad (1)$$

where, ρ_g = density of the glass, g/cm^3

ρ_l = density of the liquid, g/cm^3

$g = 9.81 \times 10^2$ cm/s^2

D = diameter of glass microsphere, cm

η = viscosity of the liquid, poise

The density of the glass is also important to sizing and screening of the glass microspheres. Glass microspheres of higher density are screened more easily than microspheres of lower density.

Screening and sizing of the glass microspheres is crucial to obtaining the proper size microsphere for this application. Handling and sizing can be done safely and easily since all separation and sizing occurs when the microspheres are non-radioactive prior to neutron activation. After neutron activation, the radioactive glass microspheres can be

transported over reasonable geographical distances with negligible loss in radiation energy.

Samarium in the form Sm_2O_3 is readily dissolved into a durable aluminosilicate glass and easily activated by neutron capture to produce the radionuclide Sm-153 (Appendix A). The radionuclide Sm-153 possesses characteristics important in treating rheumatoid arthritis.[12] The half life of Sm-153 is 46.3 h with a maximum range (LET) of 2.3 mm, an average range (LET) of 0.8 mm in human tissue, and a decay energy (beta-emission) of 0.801 MeV.[11] The range (LET) for beta emissions from Sm-153 in tissue is desirable for irradiating diseased tissue in smaller joints such as the phalanges, the wrist and the knee. The relatively small range (LET) ensures localized radiation without harming nearby healthy tissue. The high percentage of beta-emission makes Sm-153 effective as a radiotherapeutic radionuclide (Appendix B). In addition, Sm-153 has sufficient gamma-ray emissions for it to be easily monitored or located by nuclear medicine imaging devices.[13]

No previous work has been done using a Sm_2O_3 containing glass as a radiation source in radiotherapy, but Sm_2O_3 has been used in a limited number of glass systems for its fluorescent properties.[17] The amount of Sm_2O_3 used in these glasses was <1%. Other glass systems containing larger amounts of Sm_2O_3 required melting temperatures above 1800°C.[18-20] No data has been reported for glasses in the Sm_2O_3 •Al_2O_3 • SiO_2 system.

The objective of this investigation was to determine the compositional limits of glass formation in the Sm_2O_3 • Al_2O_3 • SiO_2 system and to evaluate specific glass properties in order to establish the feasibility of using such glasses for irradiating arthritic joints. Only Sm_2O_3 • Al_2O_3 • SiO_2 compositions melting below 1600°C were studied. The density, refractive

index, thermal expansion, microhardness, and chemical dissolution were measured for most compositions. Glass microspheres were made from a few selected compositions for the purpose of determining spheroidization feasibility and for use in experiments concerned with the treatment of rheumatoid arthritis.

II. EXPERIMENTAL PROCEDURE

A. GLASS MELTING

All of the $Sm_2O_3 \cdot Al_2O_3 \cdot SiO_2$ compositions investigated are listed in Table II. The raw materials (Sm_2O_3, Al_2O_3, and SiO_2)* were thoroughly dry mixed until homogeneous, and then heated, in 25 or 50 g batches in a platinum crucible in an electric furnace** to above the melting point of the mixture. Each melt was held between 1500 and 1600°C for 6-8 h to ensure homogeneity and to allow time for fining. After casting the melt into steel molds to form glass bars measuring 2 x 2 x 6 cm, the bars were annealed at 800°C for 4 h and then slowly cooled to room temperature. The glass remaining in the crucible was quenched in water, removed from the crucible and saved for property measurements. Each bar was checked for residual stress after annealing using polarized light, and any bar containing detectable residual stress was re-annealed at a higher temperature.

B. PROPERTY MEASUREMENTS

The density of each glass was measured by the Archimedian method using water as the suspending medium. The bulk density, ρ_B, of annealed, bubble free glass samples was calculated from

---

* Aesar, Johnson and Matthey, Inc., Seabrook, N.H., USA; Fisher Scientific Co., Fairlawn, N.J., USA; Particle Processing and Classifying Corp.

** Bottom Loading Rapid Temp. Furnace, Model K-BL-1700S, CM Furnaces, Inc., Bloomfield, N.J., USA.

$$\rho_B = \left[\frac{W_D}{W_D - W_S}\right]\rho_M \quad \ldots\ldots\ldots\ldots\ldots\ldots\ldots\ldots \quad (2)$$

where W_D = dry weight

W_S = suspended weight

ρ_M = density of water

The uncertainty in the measured density is $\pm$ 0.05 g/cm^3.

The refractive index of each glass was measured by the Becke line method using calibrated refractive index liquids* and a white light filter** which transmitted light at the sodium D line (589 nm). The measured refractive index has an uncertainty of $\pm$ 0.004.

The thermal expansion coefficient (α), transformation temperature (T_g), and the dilatometric softening temperature (T_d) were measured with an automatic recording dilatometer.*** Samples one inch in length were heated in air at 5°C/min. The thermal expansion was calculated from

$$\alpha = \frac{\Delta l}{l \cdot \Delta T} \quad \ldots\ldots\ldots\ldots\ldots\ldots\ldots\ldots\ldots\ldots \quad (3)$$

where Δl = change in specimen length

l = original specimen length

ΔT= temperature range (where the slope is constant)

---

* Refractive Index Liquids - R.P. Cargille Laboratories, Inc., Cedar Grove, N.J., USA.

** Filters - Interference Filters, The Ealing Corp., Cambridge, MA., USA.

*** Automatic Recording Dilatometer, The Edward Orton, Jr. Ceramic Foundation, Westerville, OH., U.S.A.

The thermal expansion coefficient of each sample was calculated from 25 to 800°C.

The Vickers Hardness Number (VHN) was measured for each glass using a microhardness tester* with a pyramid shaped diamond indentor. A load of 100 g was applied for 10 s to a sample whose surface had been polished with 1 μm alumina powder. At least 10 indentations were made on each sample, using the average indentation diagonal length to calculate the VHN in GPa. The VHN was calculated from

$$VHN = \frac{18.19 \times P}{d^2} \quad \ldots\ldots\ldots\ldots\ldots\ldots\ldots\ldots\ldots\ldots \quad (4)$$

where P = load (g)

d = the average indentation diagonal length (μm)

Slabs of known dimensions and weight were cut from a glass bar and placed in polyethylene bottles containing 100 ml deionized water. The bottles containing the as-cut glass slabs were placed in an oven at 37°C, the temperature of the human body, and agitated periodically. The slabs were removed, rinsed in deionized water, dried and weighed several times over a period of 120 days. The dissolution rate for each glass was calculated from

$$D = \frac{W_i - W}{A \cdot t} \quad \ldots\ldots\ldots\ldots\ldots\ldots\ldots\ldots\ldots\ldots \quad (5)$$

where W_i= initial weight of the glass slab

W = weight of the glass slab at time t

A = surface area of the glass slab

t = time

---

* Microhardness Tester, C. Reichert Optische Werke, Vienna, Austria.

Since the weight loss was quite small (< 0.1 mg) for the glass slabs in deionized water at 37°C, a few samples were tested in 50 ml of 1N HCl at 37°C. The weight loss was measured at 1, 7 and 14 days. Additional samples were tested in 100 ml of deionized water at 70°C. The weight loss was measured at 1, 10 and 30 days.

Slabs immersed in deionized water were removed at 10, 60 and 120 days for surface examination by SEM microscopy. Slabs immersed in 1N HCl at 37°C and deionized water at 70°C were removed after 1, 7 and 14 days and 1, 10 and 30 days, respectively, for surface examination by SEM microscopy.

Several glass compositions were crystallized in air in an electric furnace. Additional crystalline samples were obtained from nonglass forming ternary compositions initially investigated. The crystalline samples were crushed to a powder and analyzed by x-ray diffraction (XRD). X-Ray diffraction (XRD) patterns were measured at a scan rate of 2 deg./min. using copper, K-α radiation, a Ni filter, and a 0.2 degree detector slit. The d-spacings and peak intensities were compared to powder diffraction files* to identify the crystalline compounds present.

C. SPHEROIDIZATION

SmAS-41 was chosen for spheroidization since it was the most refractory glass and the other glasses were expected to form glass spheres more readily. Fifty g of SmAS-41 glass was crushed in a steel mortar and pestle and ground to a minus 400 mesh powder. A magnet was used to remove any steel fragments introduced from the crushing. The glass

---

* Fink's Index for Powder Diffraction of Inorganic Phases.

powder was fed to a oxygen propane flame sprayer* via a nitrogen carrier gas as shown in Appendix C. The glass microspheres were removed from a stainless steel tube, placed in 100 ml of methanol in a glass beaker and sonically cleaned to remove all bumps and submicrometer fragments. The glass microspheres were subsequently dried and examined by SEM microscopy.

---

* Bethlehem Burner, Bethlehem, New Hampshire.

III. RESULTS AND DISCUSSION

A. GLASS FORMATION

The region of glass formation for the $Sm_2O_3 \cdot Al_2O_3 \cdot SiO_2$ (SmAS) compositions is shown in Fig. 1 and Table II. Twenty-three of the forty-five SmAS compositions investigated formed a homogeneous, gold colored glass below 1600°C. Glass formation in the SmAS system occurred within the compositional range (8-25) $Sm_2O_3 \cdot$ (10-35) $Al_2O_3 \cdot$ (40-75) SiO_2 (mole %) for compositions melting below 1600°C. Homogeneous, bubble free glasses formed easily within this compositional range. The melts had a viscosity like that of honey, which is expected in silicate glasses where the SiO_2 content exceeds 50 mole % and no alkali is present.

Fifteen of the SmAS compositions melted below 1600°C, but remained cloudy even after 6-8 h of fining. These SmAS compositions were considered to be inhomogeneous upon cooling to room temperature as streaks of a cloudy phase were noticed. It is possible that these compositions may be phase separated, but evidence of phase separation was not found in this study. The melts became cloudy when the Sm_2O_3 content exceeded 25 mole %, the Al_2O_3 content exceeded 35 mole %, or the SiO_2 content exceeded 70 mole %.

Seven SmAS compositions did not melt below 1600°C resulting in no glass formation. The absence of glass formation in these compositions is primarily due to the high concentration of Sm_2O_3 and Al_2O_3 which exceeded 40 mole %. This result is not unusual since the melting points of Sm_2O_3 (>2300°C) and Al_2O_3 (2050°C) are significantly higher than the 1600°C maximum used in this study. Additionally, compositions exceeding

70 mole % SiO_2 yielded little glass because of the melting point of SiO_2 (1730°C).

B. PROPERTIES

1. Density. The density of the SmAS glasses varied from a low of 3.36 to a high of 4.61 g/cm^3 (Table III). Density increased linearly with increasing Sm_2O_3 content (Fig. 2). Since the density of a glass is primarily a function of the molecular weights of the oxides, it is evident that the controlling factor in these glasses is the Sm_2O_3 content whose molecular weight (348.78 g/mole) is more than three times that of Al_2O_3 (101.96 g/mole) and nearly six times that of SiO_2 (60.09 g/mole).

The density of various aluminosilicate and aluminoborate glasses are compared in Fig. 3. A higher density is obtained when oxides of high molecular weight are present in the glass. Glasses containing Sm_2O_3 have a higher density than glasses containing equivalent amounts of Y_2O_3. This trend agrees with the fact that Sm_2O_3 has a larger molecular weight than Y_2O_3 (225.8 g/mole). Yttrium oxide has a molecular weight twice that of Al_2O_3 and nearly four times that of SiO_2 and B_2O_3 (69.9 g/mole). Thus, in the SmAS, YAS (REF. 10) and YAB (REF. 21) glasses, Sm_2O_3 or Y_2O_3 additions yield a linear increase in the density.

The density data for the YASB (REF. 22) glasses in Fig. 3 indicate that substituting SiO_2 for B_2O_3 yields a constant density when the Y_2O_3 content is 20 mole %.

2. Refractive Index. The refractive index of the SmAS glasses varied from a low of 1.598 to a high of 1.738 (Table IV). The refractive index increased with increasing Sm_2O_3 content (Fig. 4), a result consistent with the known relationship between the refractive index and the density of a glass. The largest increase in refractive index occurred when the Sm_2O_3

content increased from 15 to 20 mole % and the Al_2O_3 content increased from 15 to 35 mole %. This increase in refractive index is not unusual since Sm_2O_3 has a greater effect on increasing the density of the glass than Al_2O_3.

Figure 5 shows that the refractive index increased as either Sm_2O_3 or Y_2O_3 is added to an aluminosilicate glass. This trend is expected as the increase in the refractive index parallels the increase in the density of the glass. The refractive index of the YASB glasses remained essentially constant since SiO_2 and B_2O_3 additions do not affect the refractive index when the glass contains appreciable Y_2O_3. Unexpectedly, the refractive index of the SmAS glasses was lower than that of the YAS glasses even though the density of the SmAS glasses is greater than that of the YAS glasses.

It was noticed that all of the SmAS glasses fluoresced a bright orange when exposed to long (300 nm) and short (100 nm) wave U.V. light. This fluorescence is directly associated with the Sm ions since Al_2O_3 and SiO_2 do not fluoresce under U.V. light. This fluorescence of a Sm_2O_3 containing glass in the UV range (200-500 nm) has been reported previously.[17]

3. Thermal Expansion. The glass transformation temperature, softening temperature, and thermal expansion coefficient of the SmAS glasses are listed in Table IV. The high T_g and T_d values demonstrate the refractoriness of the SmAS glasses. An increase in the thermal expansion coefficient with increasing Sm_2O_3 content, especially between 10 to 20 mole % Sm_2O_3 is illustrated in Fig. 6.

A similar trend of an increasing thermal expansion coefficient with an increase in Sm_2O_3 or Y_2O_3 content is illustrated in Fig. 7. The SmAS glasses have a thermal expansion coefficient greater than that of YAS

glasses. The SmAS glasses containing more than 20 mole % Sm_2O_3 have a higher thermal expansion coefficient than comparable YAB and YASB glasses. The average thermal expansion coefficient for the YAB and YASB glasses is, in general, higher than that of the SmAS glasses, especially below 20 mole % Sm_2O_3. There is a slight decrease in the thermal expansion coefficient of the YASB glasses as SiO_2 is substituted for B_2O_3.

4. Vickers Hardness Number (VHN). The VHN of the SmAS glasses varied from a low of 6.55 to a high of 7.57 GPa as listed in Table III. The VHN increased with increasing Sm_2O_3 or Y_2O_3 content (Fig. 8). The increase in VHN follows the same trend as the density, although there is not necessarily a direct correlation between VHN and density. The SmAS glasses have a higher VHN than fused silica (VHN of 5.9 GPa)[23] and soda-lime silica window glass (VHN of 5.41 GPa (Table III)). It is known that Al_2O_3 is second only to diamond on the Moh's hardness scale. Since Sm_2O_3 substituted for SiO_2 with the Al_2O_3 content held constant, gave an increase in the VHN, it appears that Sm_2O_3 is a least as hard as SiO_2, but not as hard as Al_2O_3. This is an approximation as there is no reported data on the hardness of Sm_2O_3.

Comparison of the VHN of the SmAS glasses to the YAS and YAB glasses (Fig. 8) reveals that Y_2O_3 substituted for SiO_2, or B_2O_3 with Al_2O_3 content constant yields a higher VHN than similar SmAS glasses. This suggests that Y_2O_3 is harder than Sm_2O_3. The VHN of the YASB glasses is lower than that of the SmAS glasses which suggests that SiO_2 replacing of B_2O_3 slightly weakens the glass structure.

5. Dissolution Rate. Table V lists the dissolution rate of the SmAS glasses immersed in deionized water (pH=6.9) at 37°C and 70°C. The dissolution rate of the SmAS glasses immersed in deionized water at 37°C

increased with increasing Sm_2O_3 content. The dissolution rate at 70°C decreased with increasing Sm_2O_3 content, an unexpected result. The dissolution rate measured for the SmAS glasses immersed in deionized water ranged from a low of 1.6 to a high of 29.9 x 10^{-9} g/cm^2·min. The weight loss was measured to ± 0.0001 g, which corresponds to a relative error in the calculated dissolution rate of ± 1.0 x 10^{-9} g/cm^2·min. Thus, only large differences in the calculated dissolution rate were used to distinguish the relative chemical durability of various glasses. SmAS-4, -6, -12, -16, -17, -37, and -41 had the lowest dissolution rates (<11.0 x 10^{-9} g/cm^2·min). SmAS-16 was the most durable glass measured in deionized water (<2.5 x 10^{-9} g/cm^2·min).

The dissolution rate of a glass can be altered by changing the temperature of the immersion liquid and the time in the immersion liquid. The SmAS glasses were immersed in deionized water at 37°C for 120 days and 70°C for 30 days. The selection of 37°C was designed to simulate the average human body temperature. The dissolution rate of SmAS glasses at 70°C was, as expected, slightly greater than that of the same glass at 37°C (Table V). The surface appearance of SmAS-12 immersed in deionized water at 37°C (Fig. 9) and 70°C (Fig. 10) shows the greater surface corrosion of SmAS-12 at 70°C for a shorter period of time. Glasses immersed at 37°C and 70°C yielded a low dissolution rate (≈ 10 x 10^{-9} g/cm^2·min) which was constant over the immersion period.

The dissolution rate of a glass can also depend on the pH of the immersion liquid. SmAS-2, -3, -4, and -6 were immersed in 1N HCl (pH=1.0) at 37°C for 14 days. The dissolution rate of the SmAS glasses immersed in 1N HCl was 100 times larger than in deionized water at 37°C and 70°C (Table VI). The surface corrosion of SmAS-4 after only 14 days in

1N HCl at 37°C is shown in Fig. 11. The large fissures seen on the surface of SmAS-4 denote chemical attack of the glass. It can be seen that the glass immersed in 1N HCl at 37°C corroded more severely in less time than the glasses immersed in deionized water at 37 °C and 70°C.

Comparison of SmAS glasses to YAS, YAB and YASB glasses (Table VI) illustrates the superior chemical durability of the SmAS glasses. At 50°C in 1N HCl, YAS-4 the most durable Y_2O_3 containing glass, was less durable than SmAS-4 at 37°C in 1N HCl. Since YAS-4 and SmAS-4 contain the equivalent mole percent Y_2O_3 and Sm_2O_3, respectively, the SmAS glasses at 37°C should be as least as durable as similar YAS glasses at 37°C. Since YAS-4 is known to be sufficiently durable for an in vivo application[8] it is expected that the SmAS glasses with greater chemical durability should also be satisfactory for in vivo applications.

A calculation of the predicted amount of Sm-153 released in vivo during the radioactive decay period of SmAS-16 can be based on the calculated dissolution rate (1.6×10^{-9} g/cm^2•min) of SmAS-16 at 37°C (Appendix B). The selection of SmAS-16 for this calculation is based on the high chemical durability and the relatively high Sm content (39 %) of the glass. It is assumed that 1 mg of 30 μm SmAS-16 microspheres are activated in the manner described in Appendix B. After 20 d in vivo, the microspheres will release 1.56×10^{21} Sm-atoms which is equivalent to 0.11 mCi/mg glass. This amount of radiation is negligible compared to the initial dose (102.5 mCi/mg glass).

The chemical durability data of the SmAS glasses indicates these glasses should be suitable for treating rheumatoid arthritis. The SmAS glasses have a high chemical durability at the physiological temperature (37°C). The chemical durability of the SmAS glasses is somewhat lower at

70°C, but this temperature is impossible in the human body. The SmAS glasses are sufficiently durable over extended periods of time (up to 120 days). This is important in keeping the glass chemically inert and insoluble for longer than the time the glass is radioactive (19 days). The SmAS glasses are less durable in 1N HCl (pH=1) at 37°C, but are quite durable at physiological values, pH 7.4 at 37°C.

6. X-Ray Diffraction (XRD). Four glasses, SmAS-12, -20, -23, and -33, and seven other compositions which did not form homogeneous glasses were analyzed by XRD (Table VII). The four glasses were crystallized using the heat treatments listed in Table VIII. The crystalline compounds identified are listed in Table VII. No ternary phases were identified and there were no unidentified phases.

Crystalline SmAS compositions containing more than 25 mole % Sm_2O_3 contained $Sm_2O_3 \cdot SiO_2$ and $Sm_2O_3 \cdot 2\ SiO_2$. XRD analysis of crystalline SmAS compositions containing more than 35 mole % Al_2O_3 contained $3\ Al_2O_3 \cdot 2\ SiO_2$ (mullite) and Al_2O_3 (corundum) or SiO_2 (cristobalite), depending on the SiO_2 content. Crystalline SmAS compositions exceeding 70 mole % SiO_2 contained $Sm_2O_3 \cdot 2\ SiO_2$ and SiO_2 (cristobalite).

The crystalline compounds listed in Table VII and the known binary phase equilibrium diagrams for $Al_2O_3 \cdot Sm_2O_3$ [24], $Sm_2O_3 \cdot SiO_2$ [25], and $Al_2O_3 \cdot SiO_2$ [26] were used to construct a tentative $Sm_2O_3 \cdot Al_2O_3 \cdot SiO_2$ ternary phase diagram (Fig. 12). The compounds determined by XRD were in good agreement with the compounds expected by correlation with the three binary systems and the composition triangles for phases determined below 1600°C. The region of glass formation appears in the temperature region below the 1600°C isotherm as expected. Since no $Sm_2O_3 \cdot Al_2O_3 \cdot$

SiO_2 phase equilibirum diagram has been reported, the proposed Sm_2O_3 • Al_2O_3 • SiO_2 ternary phases diagram extends the knowledge of the three combined binary phase equilibrium diagrams. Complete equilibrium is required of all crystalline phases in a phase equilibrium diagram. The postulated diagram (Fig. 12) is presented only as a compatability phase diagram.

7. Glass Structure. For the region of glass formation in the Sm_2O_3 • Al_2O_3 • SiO_2 system, no measurements were made to determine the glass structure. However, a general theory for the structure of the SmAS glasses may be hypothesized based on known information.

Silica is known to act as a glass forming oxide and Al_2O_3 is treated as an intermediate glass forming oxide. This classification was made based on the single-bond strength of each oxide and Zachariasen's rules for glass forming oxides.[27] Samaria in 6-fold coordination would be treated as a network modifier if based solely on the single-bond strength of Sm-O (25 k cal/mole).[28] However, evidence for Sm_2O_3 behaving as a glass forming oxide lies in the fact that glass formation occurred in SmAS compositions with a SiO_2 content as low as 16 weight % and Sm_2O_3 content as high as 63 weight %. It is unlikely that a glass would form in a system with such a high modifier content.

In a study of the structure of a 20 Al_2O_3 • 80 SiO_2 (mole %) glass using Nuclear Magnetic Resonance (NMR) [29], Si was determined to be in 4-fold coordination and Al was determined to exist in 4 and 6-fold coordination. The differentiation of the existence of Al in 4 or 6-fold coordination was not determined in the present study. Silicon is known to exist in 4-fold coordination as (SiO_4) tetrahedra. The radius ratio rule suggests that Al and Sm would be in 4-fold and 6-fold coordination,

respectively, and would be present in the glass as (AlO_4) tetrahedral groups and (SmO_6) octahedral groups, respectively. The existence of Sm in 6-fold coordination is not unexpected since it can be found in 6-fold coordination in the perovskite crystal structure ($SmAlO_3$) seen in the $Sm_2O_3 \cdot Al_2O_3$ binary phase equilibrium diagram.[24]

The hypothesized structure of the SmAS glasses contains four possible structural groups: (SiO_4), (AlO_4), (AlO_6) and (SmO_6). This structure describes a three-dimensional glass structure that is in good agreement with the information now available. It would be of interest to study the structure of these glasses by NMR or other techniques.

C. SPHEROIDIZATION

The SmAS-41 glass, which has the highest Sm_2O_3 and Al_2O_3 content of any of the glasses formed, was crushed to minus 400 mesh and spheroidized in the manner depicted in Appendix C. As the powder enters the flame a molten particle is formed. Surface tension draws the molten particle into a molten sphere. Rapid cooling upon exiting the flame allows for the formation of glass microspheres. Glass microspheres were easily formed and are shown in Fig. 13. This glass formed solid glass microspheres which were easily sized and separated. Successful spheroidization of SmAS-41 demonstrates the ability to form glass microspheres from SmAS glass compositions.

IV. CONCLUSIONS

The $Sm_2O_3 \cdot Al_2O_3 \cdot SiO_2$ system contains a large region of glass formation below 1600°C. The compositional range for glass formation lies within (10-25) Sm_2O_3 • (20-35) Al_2O_3 • (40-75) SiO_2 (mole %) and solid spheres could be easily formed from these glasses.

The density, refractive index, and microhardness of the SmAS glasses tend to increase with increasing Sm_2O_3 content up to 25 mole %. The density, refractive index, and microhardness are higher than that of fused silica. The SmAS glasses are fairly refractory, with a T_g varying from ≈ 780 to 825°C depending on composition. The thermal expansion coefficient of the SmAS glasses is relatively high compared to their T_g values. Glasses with a high T_g value tend to have a low thermal expansion coefficient. The chemical durability of the SmAS glasses is high in deionized water at 37°C and 70°C, but is lower in 1N HCl at 37°C.

The structure of the SmAS glass is postulated to consist of four structural groups: (SiO_4), (AlO_4), (AlO_6), and (SmO_6). Samaria is believed to behave as a glass forming oxide.

The SmAS glasses are sufficiently durable and chemically inert beyond the effective radioactive life of Sm-153 to permit usage in treating rheumatoid arthritis. The chemical durability of the SmAS glasses is higher than that of the YAS glasses which have already proven to be satisfactory for use in the human body. The radiation characteristics of Sm-153 are excellent for use in treating rheumatoid arthritis. The high density of the SmAS glasses permit easy screening of the glass microspheres.

Several of the SmAS glasses have excellent properties for the use in the treatment of rheumatoid arthritis. The flexibility of having several different glass compositions to choose from is an advantage when a single glass composition must be selected for the treatment of rheumatoid arthritis. An excellent starting composition is SmAS-16 (14 Sm_2O_3 • 16 Al_2O_3 • 70 SiO_2 (mole %)), which has the highest chemical durability.

REFERENCES

1. J. Minckler, H. B. Anstall, T. M. Minckler, (pg. 215), Pathobiology an Introduction, The C.V. Mosby Company, St. Louis, 1971.

2. J. M. Gumpel and N.C. Roles, "A Controlled Trial of Intra-Articular Radiocolloids versus Surgical Synovectomy in Persistent Synovitis," The Lancet, 1, 488-489 (1975).

3. E. D. Grady, "Internal Radiation Therapy of Hepatic Cancer," Diseases of the Colon and Rectum, Vol. 22, No. 6, (September, 1979).

4. J. F. Bridgeman et al., "Irradiation of the Synovium in the Treatment of Rheumatoid Arthritis," Quarterly Journal of Medicine, New Series, 166, 357-367 (1973).

5. J. Ingrand, "Characteristics of Radio-Isotopes for Intra-articular Therapy," Ann. Rheum. Dis., 32 Suppl. 2-9, (1973).

6. L. Rosenthall, "Use of Radiocolloids for Intra-Articular Therapy for Synovitis," 147-153, Therapy in Nuclear Medicine, R.P. Spencer, ed., Grune and Stratton, New York, (1978).

7. C. B. Sledge et al., "Treatment of Rheumatoid Synovitis of the Knee with Intra-articular Injection of Dysprosium 165-Ferric Hydroxide Macroaggregates," 29, 153-159 (1986).

8. G. J. Ehrhardt and D.E. Day, "Therapeutic Use of ^{90}Y Microspheres," Nucl. Med. Biol., 14, 233-242, (1987).

9. R. J. Glanchard, "Precautions in the Use of ^{90}Y Microspheres," 32, 367-370, Ann. of Int. Med., (1976).

10. M.J. Hyatt and D.E. Day, "Glass Properties in the Yttria•Alumina•Silica System," J. Am. Ceram. Soc., 70 [10], C283-287, (1987).

11. CRC-Handbook of Radioactive Nuclides. Part 1, The Chemical Rubber Co. Handbook Series, Y. Wang, ed., Cleveland, Ohio. (1969).

12. G. Henesy, Radioactive Indicators: Their Application in Biochemistry, Animal Physiology, and Pathology, Interscience Publishers, Inc. New York (1948).

13. W.E. Siri, Isotopic Tracers and Nuclear Radiations with Applications in Biology and Medicine, Ch.7 McGraw-Hill Book Co., Inc. York, PA (1949).

14. M.D. Glascock, "Neutron Activation Analysis Tables," Research Reactor Facility University of Missouri-Columbia, Columbia, MO (1985).

15. CRC - Techniques of Biocompatability Testing, Vol. J., pg.14, CRC Series in Biocompatability, D.F. Williams, ed., CRC Press, Inc. Boca Raton, Florida (1968).

16. J. T. Jones, M. F. Berard, Ceramics Industrial Processing and Testing, pg. 143, The Iowa State University Press, Ames, Iowa (1972).

17. T. Takahashi and O. Yamada, "Fluorescent Properties of Alkali and Alkaline Earth Rate Earth Metaphosphate Glass Phosphors," RCA Review, Vol. 41, 65-91, (March, 1980).

18. S. Yajima, K. Okamura, and T. Shishido, "Formation of Unusual Glasses Based on Ln_2O_3," 11th Rare Earth Research Conference, Vol. 11, 568-577, (October, 1974).

19. L.E. Topol and R.A. Happe,"Formation of New Lanthanide Oxide Glasses by Laser Spin Melting and Free Fall Cooling," J. of Non. Cryst. Solids, 15, 116-124, (1974).

20. B. V. Janakirama-Rao, "Alkaline Earth Oxide/Fluoride-Rare Earth Oxide-Silicon Dioxide Glass Compositions," United States Patent #3,468,682, Sept.,1969.

21. H. L. Rutz and C. F. Spencer, Jr., "Property Survey of Glasses in the $B_2O_3 \cdot Al_2O_3 \cdot Y_2O_3$ System," Unpublished work, University of Missouri-Rolla (1985).

22. A. L. Applewhite, "Property Survey of $Y_2O_3 \cdot Al_2O_3 \cdot SiO_2 \cdot M_xO_y$ Glasses," M.S. Thesis, University of Missouri-Rolla (1987).

23. Physical Sciences Data, Vol. 15., Handbook of Glass Data, Part A; pg. 144, "Silica and Binary Silicate Glasses," O.V. Mazurin, M.V. Streltsina and T. P. Shvaiko-Shvaikovskaya, eds., Elsevier Science Publishers, B.V., Amsterdam (1983).

24. S. J.Schneider, R. S. Roth, and J. L. Waring, J. Research Natl. Bur. Standards, 65A [4] 364 (1961).

25. N. A. Toropov, Trans. Intern. Ceram. Congr., 7th London, 1960, p. 439; N. A. Toropov and L. A. Bondar, Izv. Nauk SSSR, Otd. Khim. Navk, No. 8, 1372 (1961); Bul. Acad. Sci. USSR, Div. Chem. Sci. (English Transl.), 1279 (1961).

26. Shigeo Aramaki and Rustum Roy, J. Am. Ceram. Soc., 42 [12] 644 (1959); ibid; 45 [5] 239 (1962).

27. W. D. Kingery, H. K. Bowen, D. R. Uhlmann, Introduction to Ceramics, 2nd Edition, Ch.2, p.99, John Wiley & Sons, New York, (1976).

28. CRC-Handbook of Chemistry and Physics, 57th Edition, F-219, R. C. Weast, ed., CRC Press, Cleveland, Ohio, (1977).

29. M. Yamane, S. Inoue, et al, "Homogeneity of $Al_2O_3 \cdot SiO_2$ Glass Prepared by Melting in an Infrared-Image Furnace," Advances in the Fusion of Glass, 51.1 - 51.11, (1988).

VITA

Erik Michael Erbe was born on February 28, 1965 in Shawnee Mission, Kansas. He received his primary and secondary education in St. Louis, Missouri. He received a Bachelor of Science Degree in Ceramic Engineering from the University of Missouri-Rolla, in Rolla, Missouri in May, 1987. He is a member of Keramos, the American Ceramic Society, National Institute of Ceramic Engineers, Missouri Academy of Science and Sigma Xi Research Society.

TABLE II

COMPOSITIONS INVESTIGATED, MELTING TEMPERATURE, AND GLASS FORMATION

Sample	(Mole %) Sm_2O_3	Al_2O_3	SiO_2	Melting Temp. °C	Glass Formation	Properties Evaluated
SmAS- 1	8.9	19.3	71.8	1550	Homog.*	NO
SmAS- 2	20.5	25.5	54.0	1540	Homog.	YES
SmAS- 3	17.1	23.4	59.5	1560	Homog.	NO
SmAS- 4	11.8	20.0	68.2	1550	Homog.	YES
SmAS- 5	6.0	16.6	77.4	1560	Cloudy †	NO
SmAS- 6	13.2	26.8	60.0	1540	Homog.	YES
SmAS- 7	12.6	32.4	55.0	1575	Cloudy	NO
SmAS- 8	11.2	12.4	76.4	1550	Cloudy	NO
SmAS- 9	19.6	18.3	62.1	1550	Homog.	NO
SmAS-10	10.6	36.4	53.0	1575	Cloudy	NO
SmAS-11	5	20	75	>1600	None	NO
SmAS-12	10	15	75	1550	Homog.	YES
SmAS-13	15	10	75	1550	Cloudy	NO
SmAS-14	20	10	70	1550	Cloudy	NO
SmAS-15	16.4	16.9	66.7	1540	Homog.	YES
SmAS-16	13.7	15.6	70.7	1550	Homog.	YES
SmAS-17	10	20	70	1540	Homog.	YES
SmAS-18	5	25	70	>1600	None	NO
SmAS-19	5	30	65	>1600	None	NO
SmAS-20	10	25	65	1550	Homog.	YES
SmAS-21	15	20	65	1540	Homog.	YES
SmAS-22	20	15	65	1550	Homog.	YES
SmAS-23	25	10	65	1575	Homog.	YES
SmAS-24	25	15	60	1550	Homog.	YES
SmAS-25	20	20	60	1550	Homog.	YES
SmAS-26	10	30	60	>1600	Cloudy	NO
SmAS-28	15	30	55	1550	Homog.	YES
SmAS-29	25	20	55	1540	Homog.	YES
SmAS-30	30	15	55	1560	Cloudy	NO
SmAS-31	30	10	60	>1600	None	NO
SmAS-32	30	20	50	>1600	None	NO
SmAS-33	25	25	50	1540	Homog.	YES
SmAS-34	20	30	50	1540	Homog.	YES
SmAS-35	27.5	7.5	65	1550	Cloudy	NO
SmAS-36	15	35	50	1575	Cloudy	NO
SmAS-37	20	35	45	1540	Homog.	YES
SmAS-38	25	30	45	1540	Homog.	YES
SmAS-39	30	25	45	1575	Cloudy	NO
SmAS-40	30	30	40	>1600	Cloudy	NO
SmAS-41	25	35	40	1550	Homog.	YES
SmAS-42	20	40	40	1550	Cloudy	NO

Table II continued...

Sample	(Mole %)			Melting	Glass	Properties
	Sm_2O_3	Al_2O_3	SiO_2	Temp. °C	Formation	Evaluated
SmAS-43	15	40	45	>1600	None	NO
SmAS-44	30	35	35	>1600	None	NO
SmAS-45	25	40	35	>1600	Cloudy	NO

* Homogeneous
† Cloudy, Inhomogeneous Melt

TABLE III

DENSITY, REFRACTIVE INDEX, AND VICKERS HARDNESS NUMBER (VHN) OF SmAS GLASSES

Glass	Density g/cm^3 (±0.05)	Refractive Index (±0.004)	VHN GPa (±0.5)
SmAS- 2	4.32	1.674	7.4
SmAS- 4	3.64	1.638	6.6
SmAS- 6	3.74	1.610	7.1
SmAS-12	3.56	1.626	-
SmAS-15	3.97	1.626	-
SmAS-16	3.84	1.610	-
SmAS-17	3.41	1.598	6.6
SmAS-20	3.36	1.610	6.7
SmAS-21	3.82	1.654	6.8
SmAS-22	4.23	1.662	-
SmAS-23	4.61	1.666	-
SmAS-24	4.61	1.658	-
SmAS-25	4.32	1.670	6.7
SmAS-28	3.83	1.670	-
SmAS-29	4.61	1.674	7.1
SmAS-33	4.59	1.682	7.6
SmAS-34	4.22	1.690	-
SmAS-37	4.19	1.708	-
SmAS-38	4.57	1.738	-
SmAS-41	4.52	1.733	-
NCS*	-	-	5.4
Fused SiO_2 (REF. 23)	2.20	1.458	5.9

* Soda-Lime-Silica

TABLE IV

GLASS COMPOSITIONS EVALUATED, TRANSFORMATION TEMPERATURE, T_g, SOFTENING TEMPERATURE, T_d, AND THERMAL EXPANSION COEFFICIENT, α.

Glass	GLASS COMPOSITION (Mole %) Sm_2O_3	Al_2O_3	SiO_2	T_g(±5°C)	T_d(±5°C)	$\alpha \times 10^7$(°C)$^{-1}$*
SmAS- 2	20.5	25.5	54.0	810	855	75.2
SmAS- 4	11.8	20.0	68.2	820	860	55.8
SmAS- 6	13.2	26.8	60.0	820	865	52.4
SmAS-12	10	15	75	810	850	51.7
SmAS-15	16.4	16.9	66.7	805	840	63.7
SmAS-16	13.7	15.6	70.7	795	840	61.9
SmAS-17	10	20	70	823	865	50.9
SmAS-20	10	25	65	825	875	53.3
SmAS-21	15	20	65	825	860	55.6
SmAS-22	20	15	65	808	875	68.3
SmAS-23	25	10	65	810	855	79.2
SmAS-24	25	15	60	780	860	69.3
SmAS-25	20	20	60	825	860	72.5
SmAS-28	15	30	55	820	845	60.4
SmAS-29	25	20	55	815	855	73.9
SmAS-33	25	25	50	808	840	78.7
SmAS-34	20	30	50	780	815	62.3
SmAS-37	20	35	45	815	855	67.5
SmAS-38	25	30	45	785	820	68.2
SmAS-41	25	35	40	815	845	66.7

* average from 25-800°C

TABLE V

DISSOLUTION RATE IN DEIONIZED WATER AT 37°C AND 70°C OF SmAS AND REFERENCE GLASSES

Glass	Dissolution Rate ($g/cm^2 \cdot min$) x 10^9 10 days	30 days	60 days	120 days
SmAS- 2	18.2	18.2	18.2	18.2
SmAS- 4	10.9	10.9	10.9	10.9
SmAS- 4*	11.4	4.8	nm	nm
SmAS- 6	5.3	3.9	3.9	3.9
SmAS- 6*	6.0	3.9	nm	nm
SmAS-12	9.3	9.3	9.3	9.3
SmAS-12*	10.6	0.9	nm	nm
SmAS-15	29.5	29.5	29.5	29.5
SmAS-16	1.6	1.6	1.6	1.6
SmAS-16*	2.3	2.3	nm	nm
SmAS-17	9.3	9.3	9.3	9.3
SmAS-17*	11.6	11.6	nm	nm
SmAS-20	23.9	23.9	23.9	23.9
SmAS-22	15.0	15.0	15.0	15.0
SmAS-23	29.7	29.7	29.7	29.7
SmAS-24	29.9	29.9	29.9	29.9
SmAS-25	16.7	16.7	16.7	16.7
SmAS-28	19.5	19.5	19.5	19.5
SmAS-29	21.2	21.2	21.2	21.2
SmAS-33	26.3	26.3	26.3	26.3
SmAS-34	21.3	21.3	21.3	21.3
SmAS-37	8.3	8.3	8.3	8.3
SmAS-37*	9.9	9.9	nm	nm
SmAS-38	14.3	14.3	14.3	14.3
SmAS-41	4.5	4.5	4.5	4.5
SmAS-41*	5.1	5.1	nm	nm
2947†	0.0	0.0	3.8	38.4
2947†*	4.6	4.6	nm	nm

nm = not measured

* Measured at 70°C. Dissolution rate was measured at 1 day but was less than 0.1 x 10^{-9} $g/cm^2 \cdot min$ in all cases.

† Corning 2947 Microslide

TABLE VI

DISSOLUTION RATE IN 1N HCl AT 37°C OF
SmAS, YAS, YAB, YASB AND REFERENCE GLASSES

Glass	(Mole%) Sm_2O_3	Al_2O_3	SiO_2	Dissolution Rate (g/cm^2-min) x 10^7 1 day	7 days	14 days
SmAS-2	20.5	25.5	54.0	46.9	28.4	23.1
SmAS-3	17.1	23.4	59.5	28.1	16.3	13.2
SmAS-4	11.8	20.0	68.2	6.2	4.2	3.2
SmAS-6	13.2	26.8	60.0	18.3	10.3	8.3
2947 *				0	0.16	0.02

* Corning 2947

Glass	(Mole%) Y_2O_3	Al_2O_3	SiO_2	B_2O_3	Dissolution Rate (g/cm^2-min) x 10^7 1 day	7 days	14 days
YAS-2 *	20.5	25.5	54.0	0	74.3	51.3	54.6
YAS-3	17.1	23.4	59.5	0	49.3	34.0	36.2
YAS-4	11.8	20.0	68.2	0	13.6	6.8	7.8
YAS-6	13.2	26.8	60.0	0	48.8	24.7	28.1
YAB-4 †	25	20	0	55	6.9	2.0	1.5
YAB-5	20	25	0	55	17.4	8.9	5.7
YASB-6 ‡	20	25	30	25	23.0	16.5	0
YASB-9	20	25	45	10	22.0	16.2	0

* YAS glasses ≈ 50°C (REF. 10)
† YAB glasses ≈ 30°C (REF. 21)
‡ YASB glasses ≈ 30°C (REF. 22)

TABLE VII

CRYSTALLINE COMPOUNDS IDENTIFIED BY XRD AND HEAT TREATMENT OF SmAS COMPOSITIONS

Sample	Heat Treatment	Compound(s) Identified
SmAS -5	1600°C for 2 h	$Sm_2O_3 \cdot 2\,SiO_2 + SiO_2$
SmAS-11	1600°C for 2 h	$Sm_2O_3 \cdot 2\,SiO_2 + SiO_2 + 3\,Al_2O_3 \cdot 2\,SiO_2$
SmAS-12	840°C for 9 h	$Sm_2O_3 \cdot 2\,SiO_2 + SiO_2$
SmAS-18	1600°C for 2 h	$3\,Al_2O_3 \cdot 2\,SiO_2 + SiO_2$
SmAS-20	865°C for 8 h	$3\,Al_2O_3 \cdot 2\,SiO_2 + SiO_2$
SmAS-23	850°C for 8 h	$Sm_2O_3 \cdot 2\,SiO_2$
SmAS-26	1600°C for 2.5 h	$3\,Al_2O_3 \cdot 2\,SiO_2 + SiO_2$
SmAS-33	830°C for 8 h	$Sm_2O_3 \cdot SiO_2 + Sm_2O_3 \cdot 2\,SiO_2$
SmAS-40	1600°C for 2 h	$Sm_2O_3 \cdot SiO_2 + Sm_2O_3 \cdot 2\,SiO_2$
SmAS-42	1600°C for 2 h	$3\,Al_2O_3 \cdot 2\,SiO_2 + Al_2O_3$
SmAS-44	1600°C for 2.5 h	$Sm_2O_3 \cdot SiO_2 + Sm_2O_3 \cdot 2\,SiO_2$

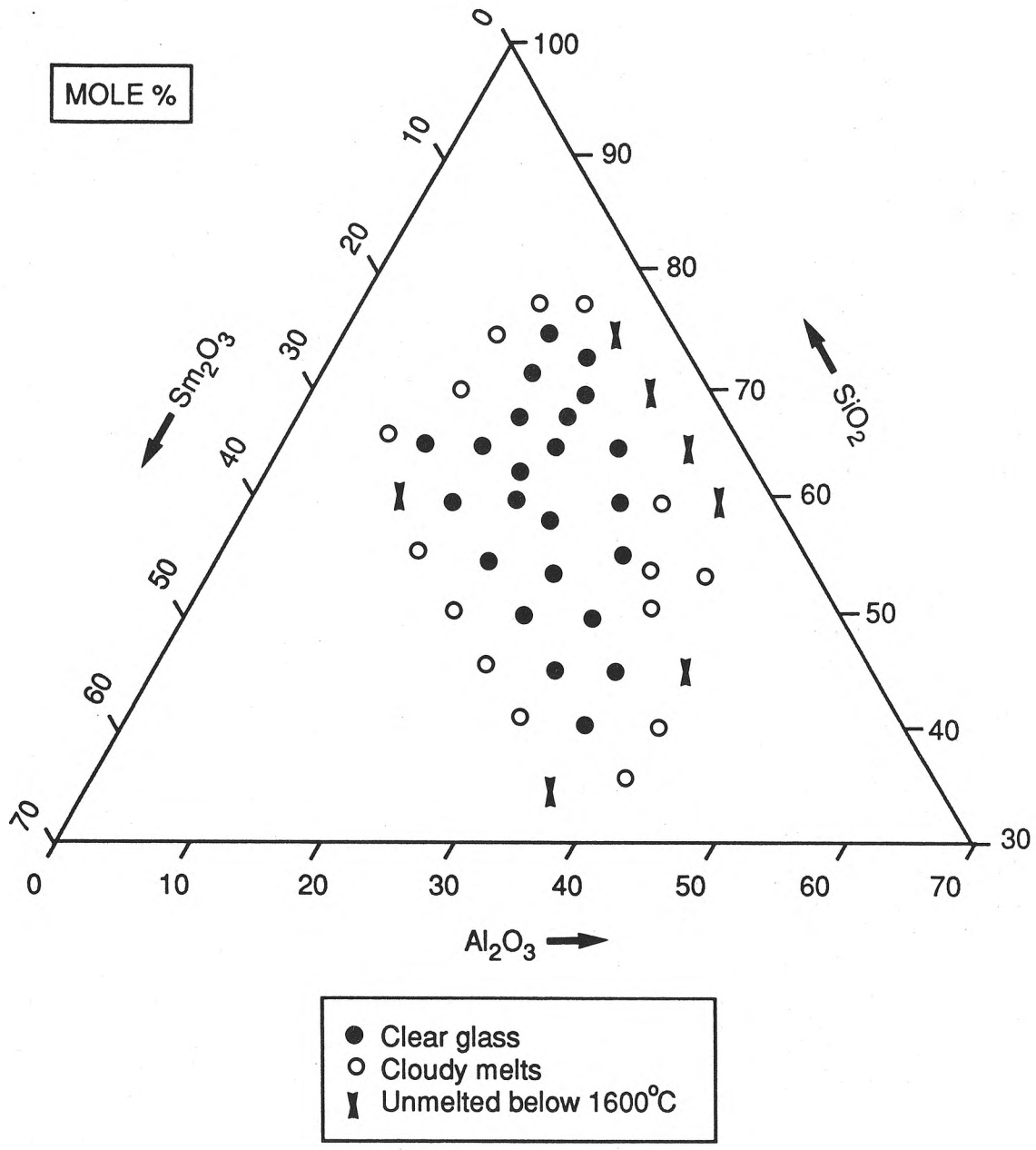

Figure 1. Diagram of the Sm_2O_3 • Al_2O_3 • SiO_2 System Showing All the Compositions Investigated and Those Forming Glass Below 1600 °C.

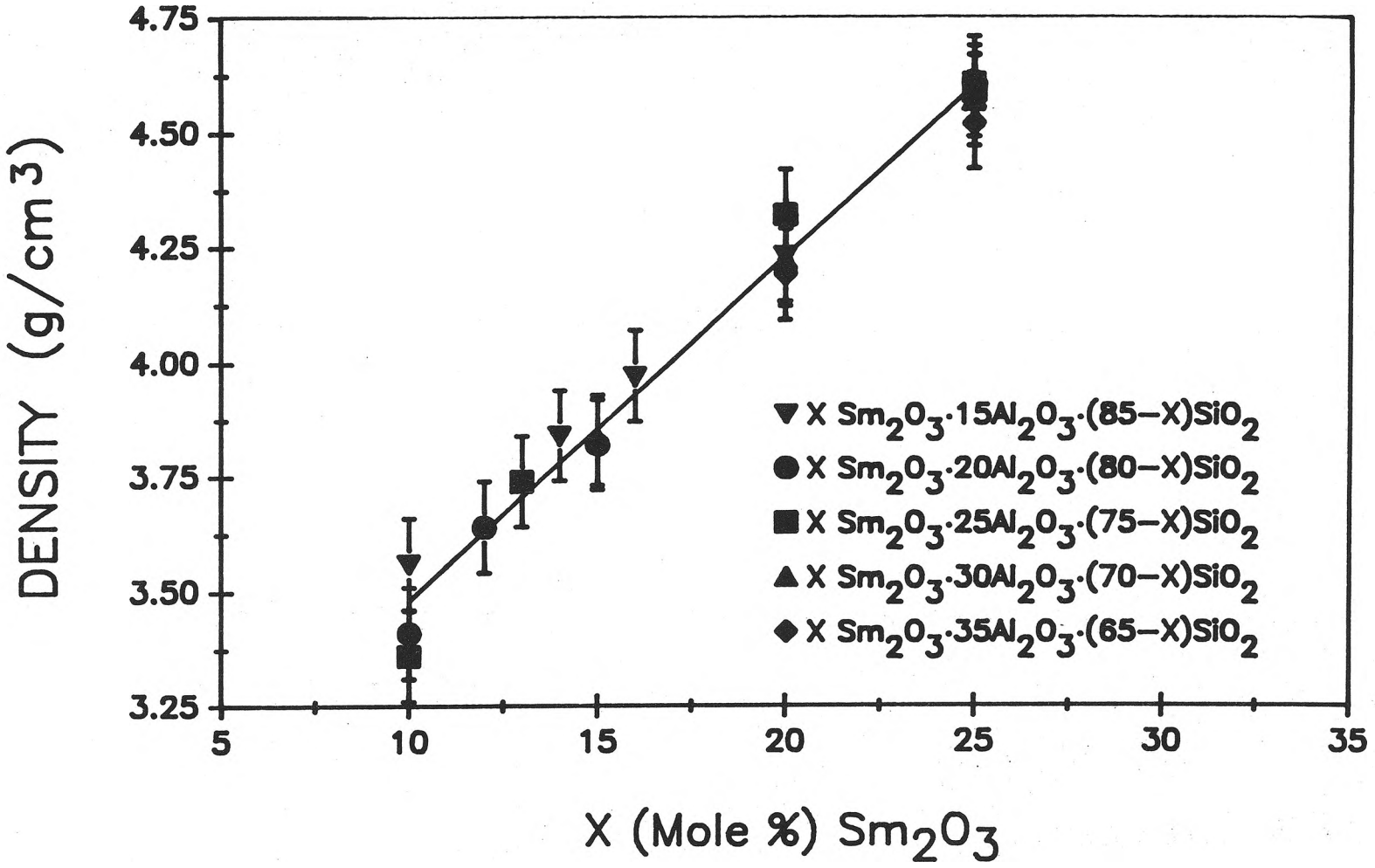

Figure 2. Density vs. Mole % Sm_2O_3 for SmAS Glasses. Density Values ± 0.05 g/cm^3.

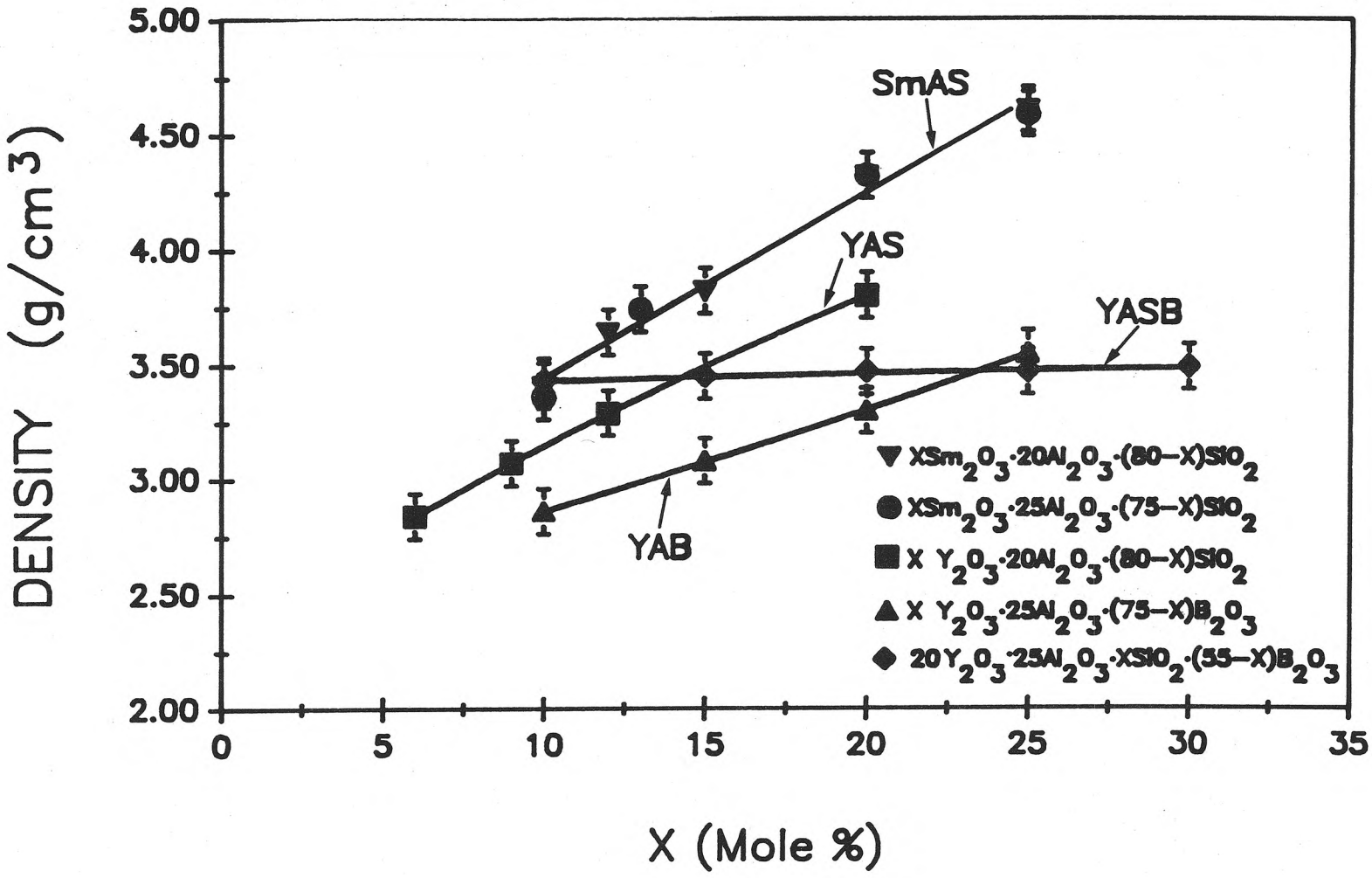

Figure 3. Density vs. Composition for SmAS, YAS (REF. 10), YAB (REF. 21) and YASB (REF. 22) Glasses. Density Values ± 0.05 g/cm^3.

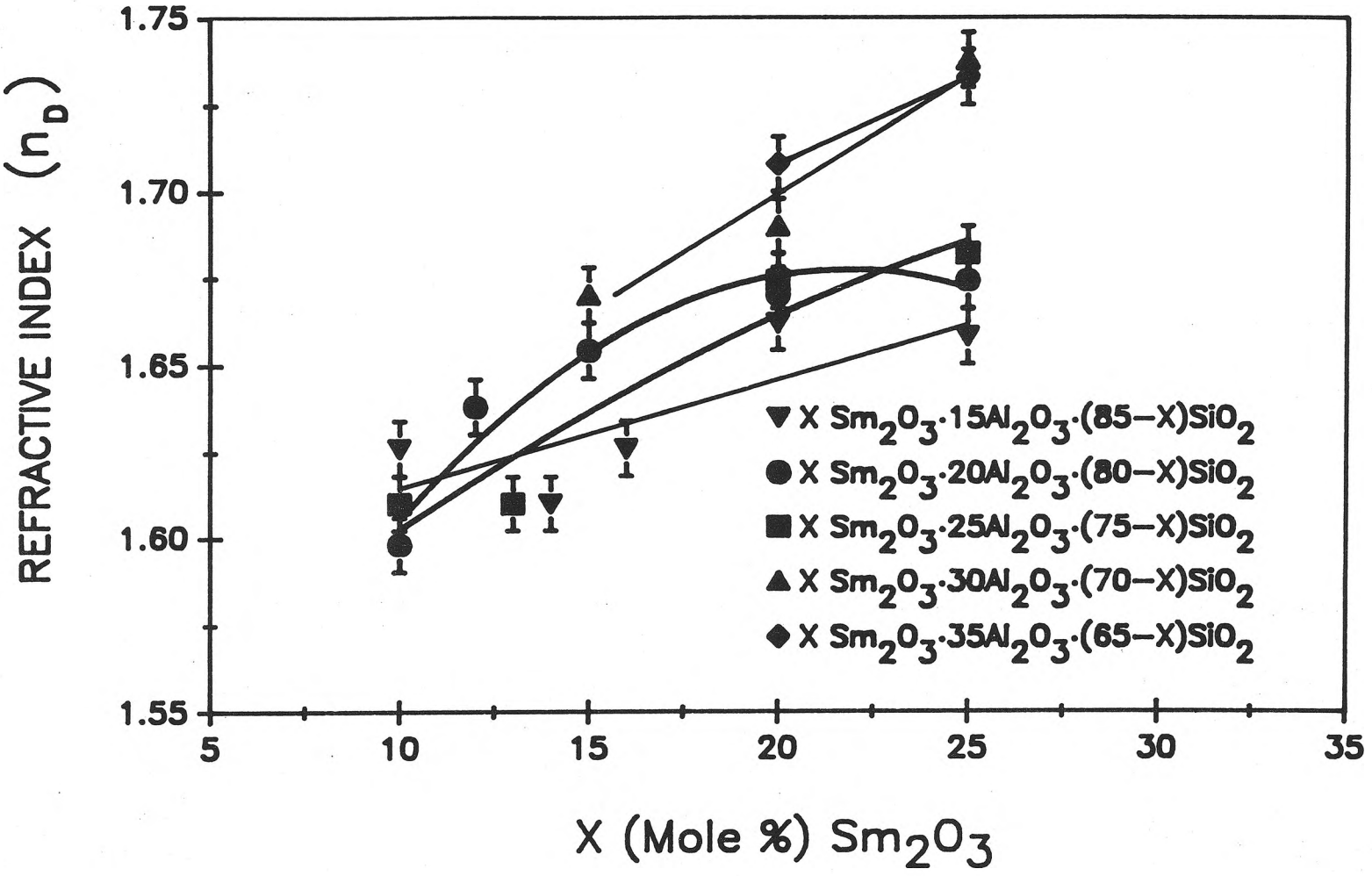

Figure 4. Refractive Index vs. Mole % Sm_2O_3 for SMAS Glasses. Refractive Index Values ±0.004.

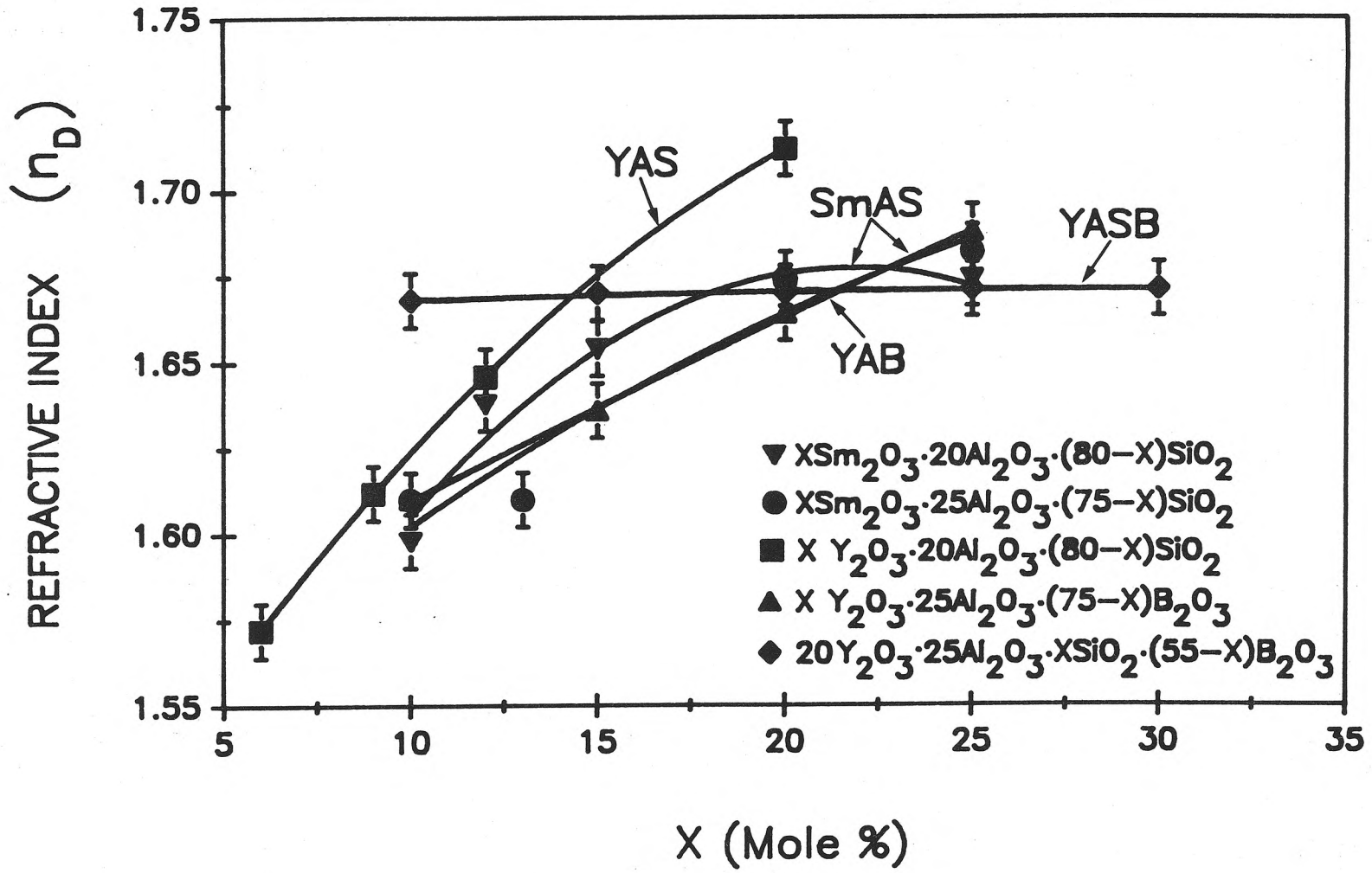

Figure 5. Refractive Index vs. Composition for SmAS, YAS (REF. 10), YAB (REF. 21) and YASB (REF. 22) Glasses. Refractive Index Values ±0.004.

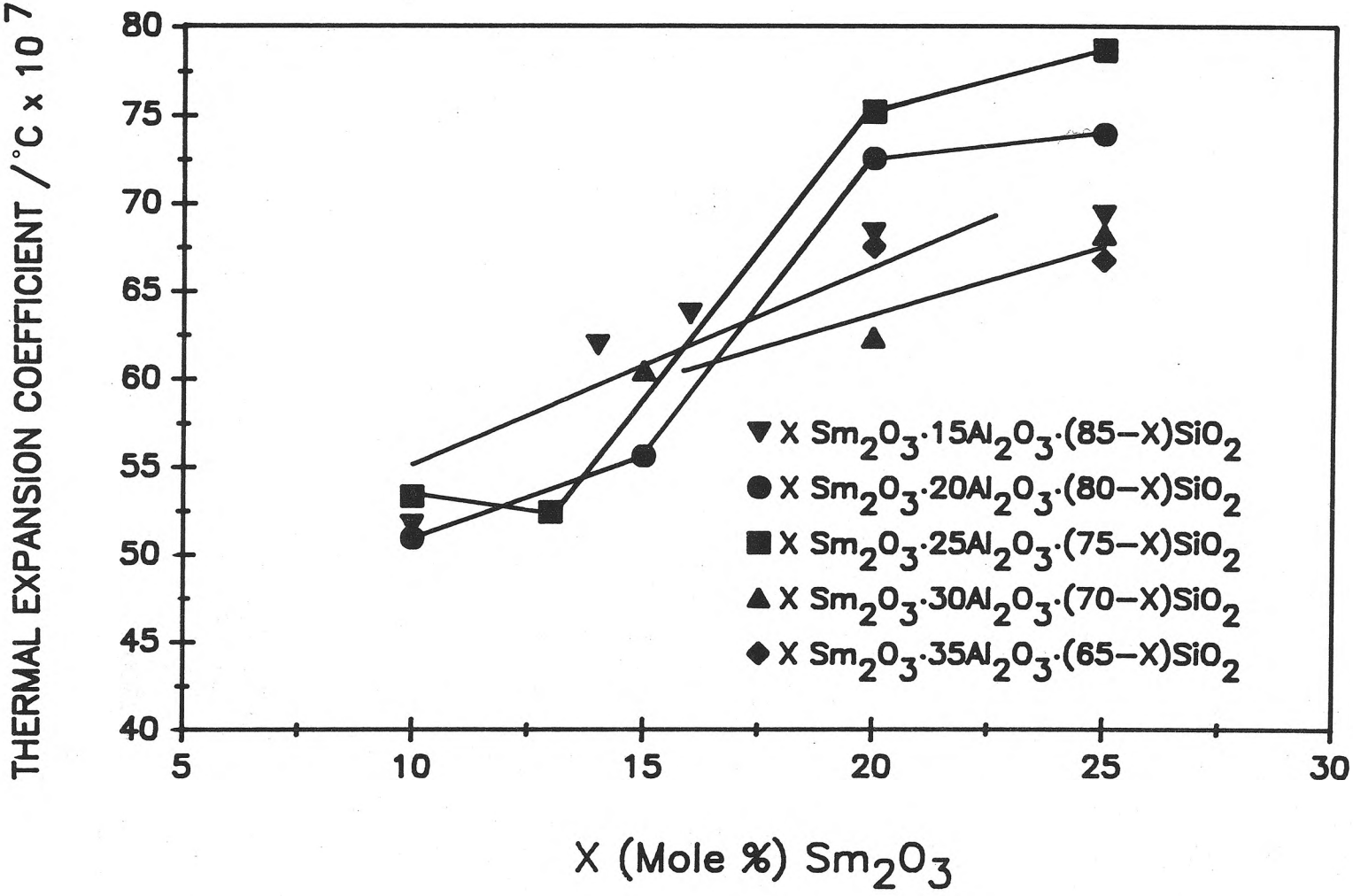

Figure 6. Thermal Expansion Coefficient vs. Mole % Sm_2O_3 for SmAS Glasses.

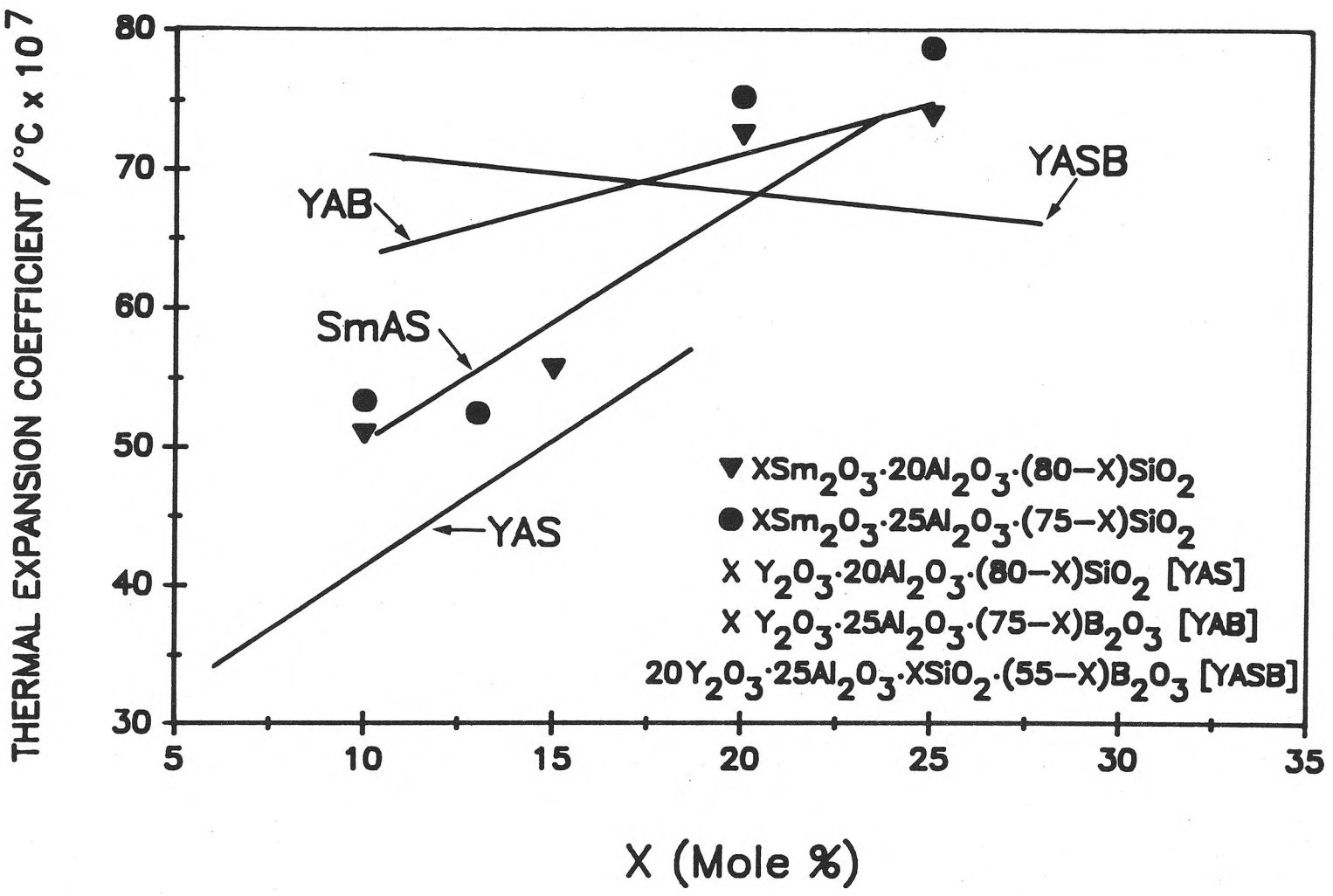

Figure 7. Thermal Expansion Coefficient vs. Composition for SmAS, YAS (REF. 10), YAB (REF. 21) and YASB (REF. 22) Glasses. Data Points for All But SmAS Glasses Are Omitted for Clarity.

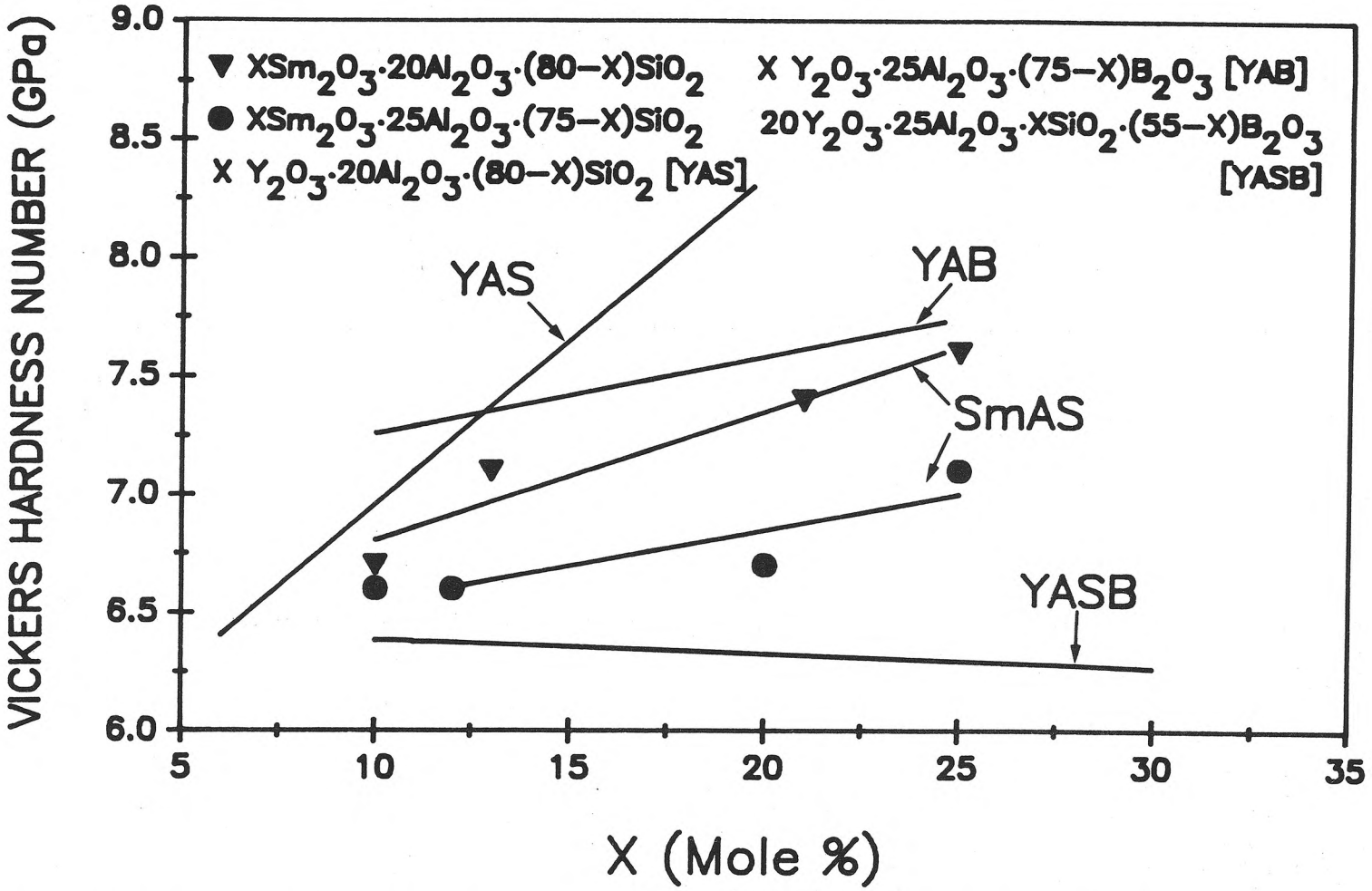

Figure 8. Vickers Hardness Number (VHN) vs. Composition for SmAS, YAS (REF. 10), YAB (REF. 21), and YASB (REF. 22) Glasses. VHN Values ±0.5 GPa. Data Points for All But SmAS Glasses Are Omitted for Clarity.

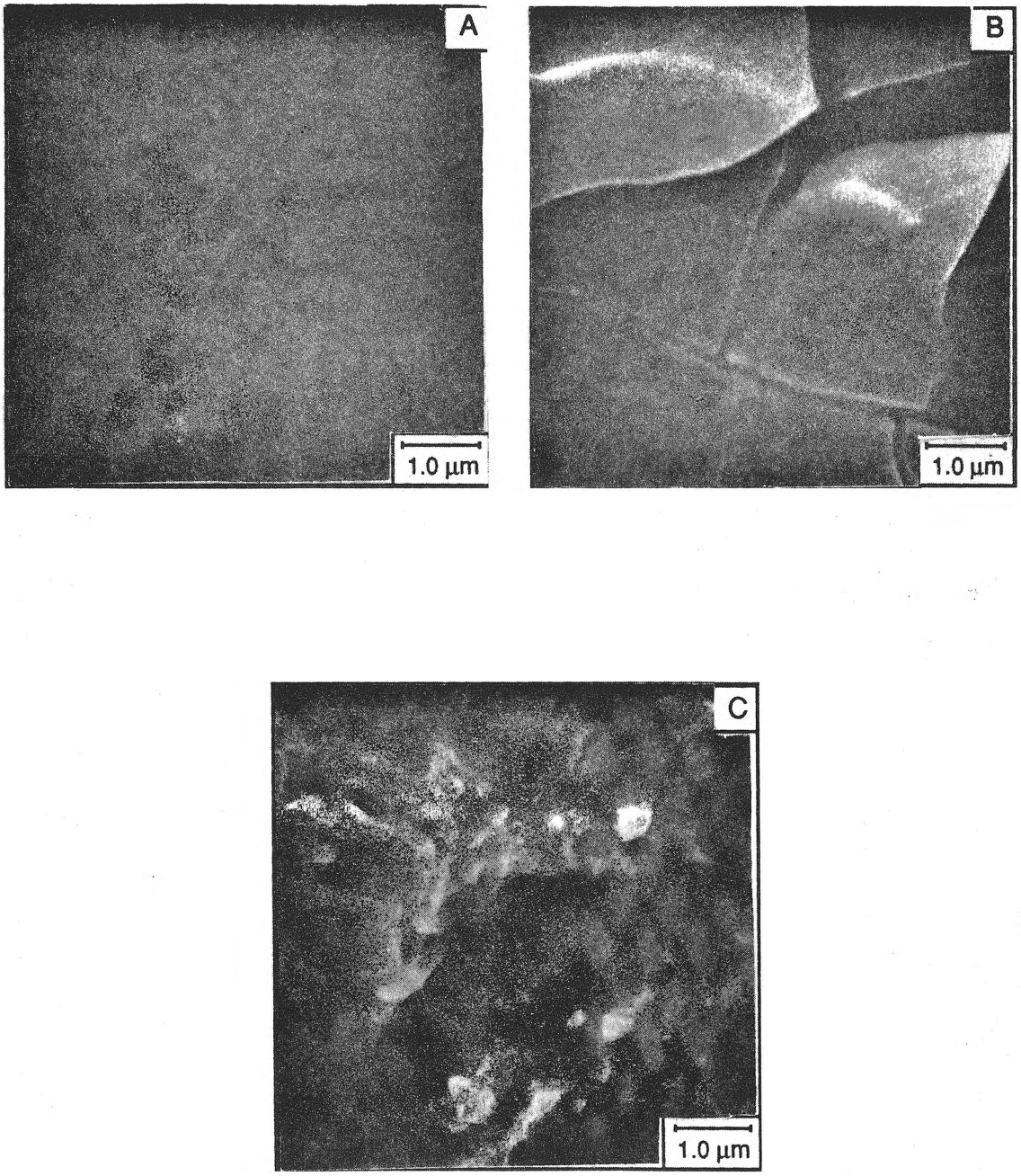

Figure 9. Surface Appearance of SmAS-12 Glass Immersed in Deionized H_2O at 37°C for A) 10, B) 60, and C) 120 Days.

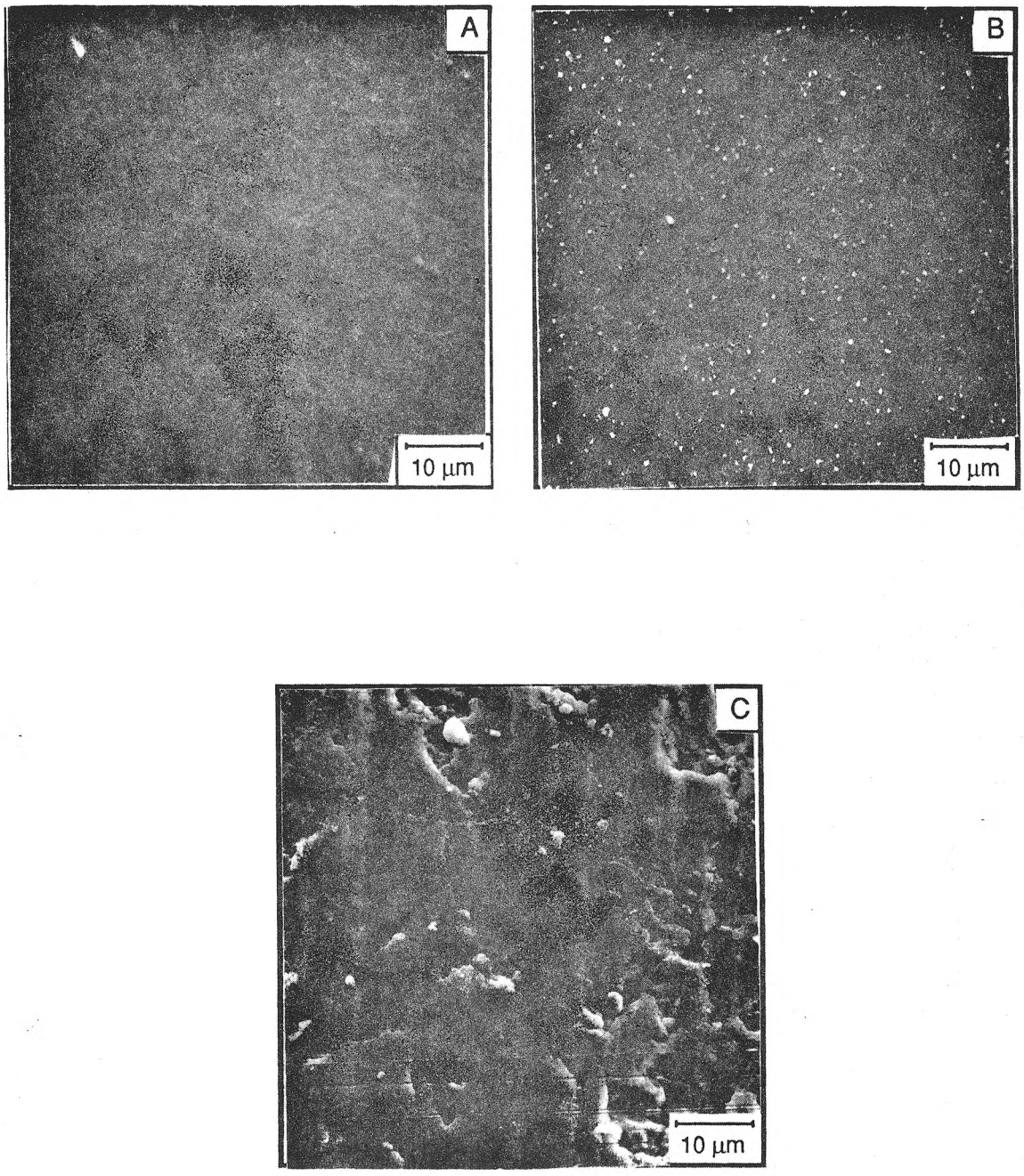

Figure 10. Surface Appearance of SmAS-12 Glass Immersed in Deionized H_2O at 70°C for A) 1, B) 10, and C) 30 Days.

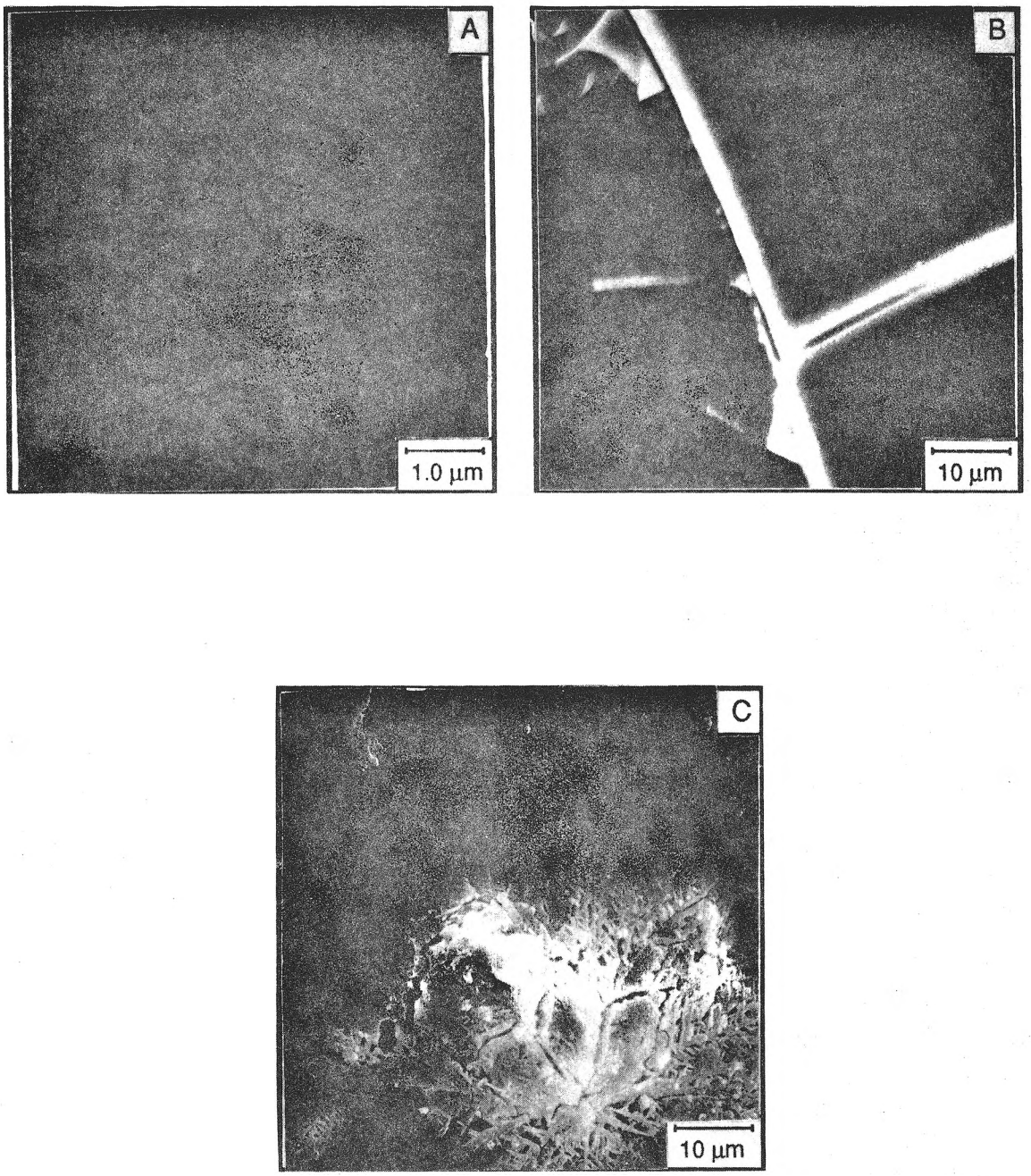

Figure 11. Surface Appearance of SmAS-4 Glass Immersed in 1N HCl at 37°C for A) 1, B) 7, and C) 14 Days.

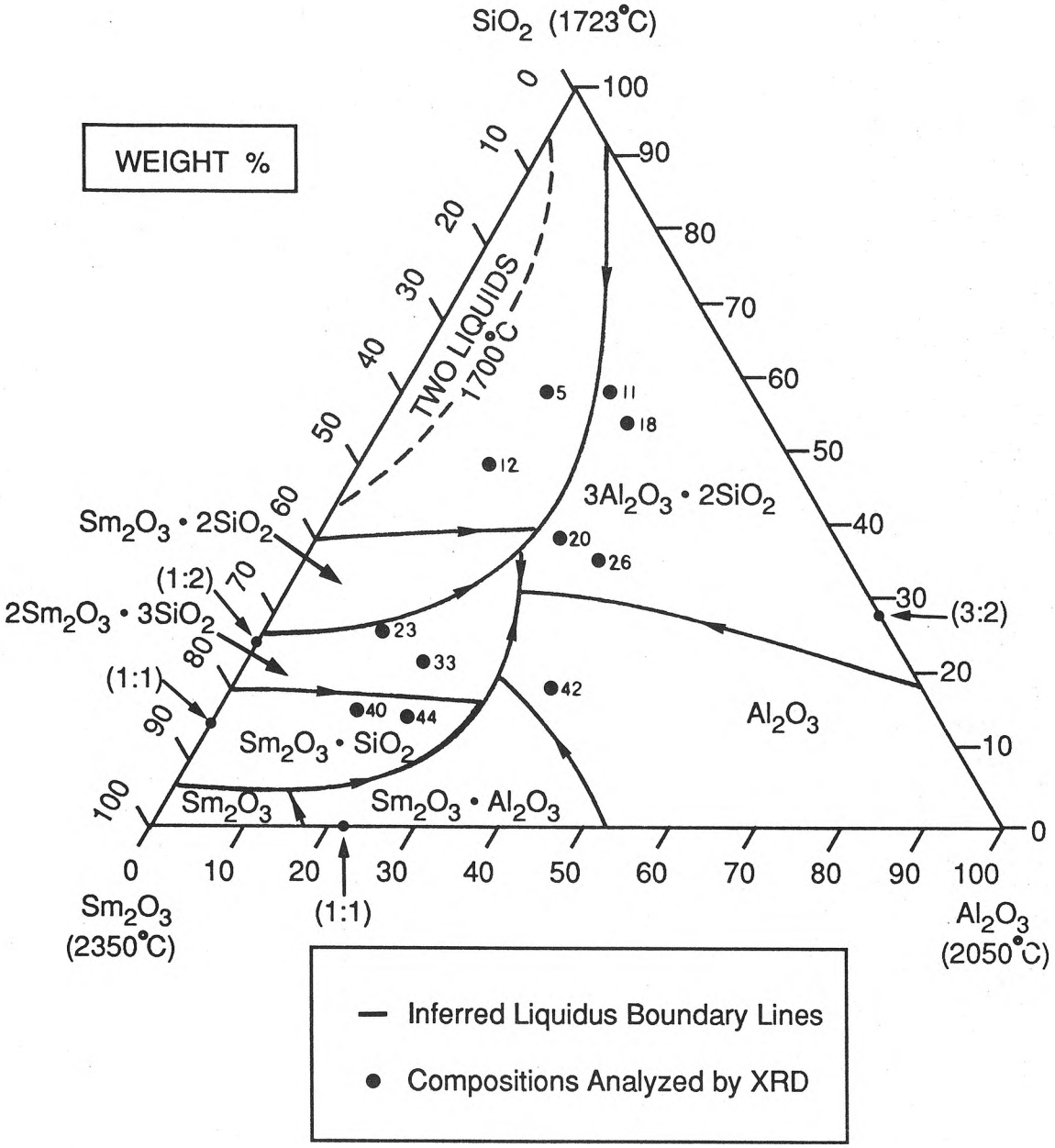

Figure 12. Proposed $Sm_2O_3 \cdot Al_2O_3 \cdot SiO_2$ Ternary Phase Diagram.

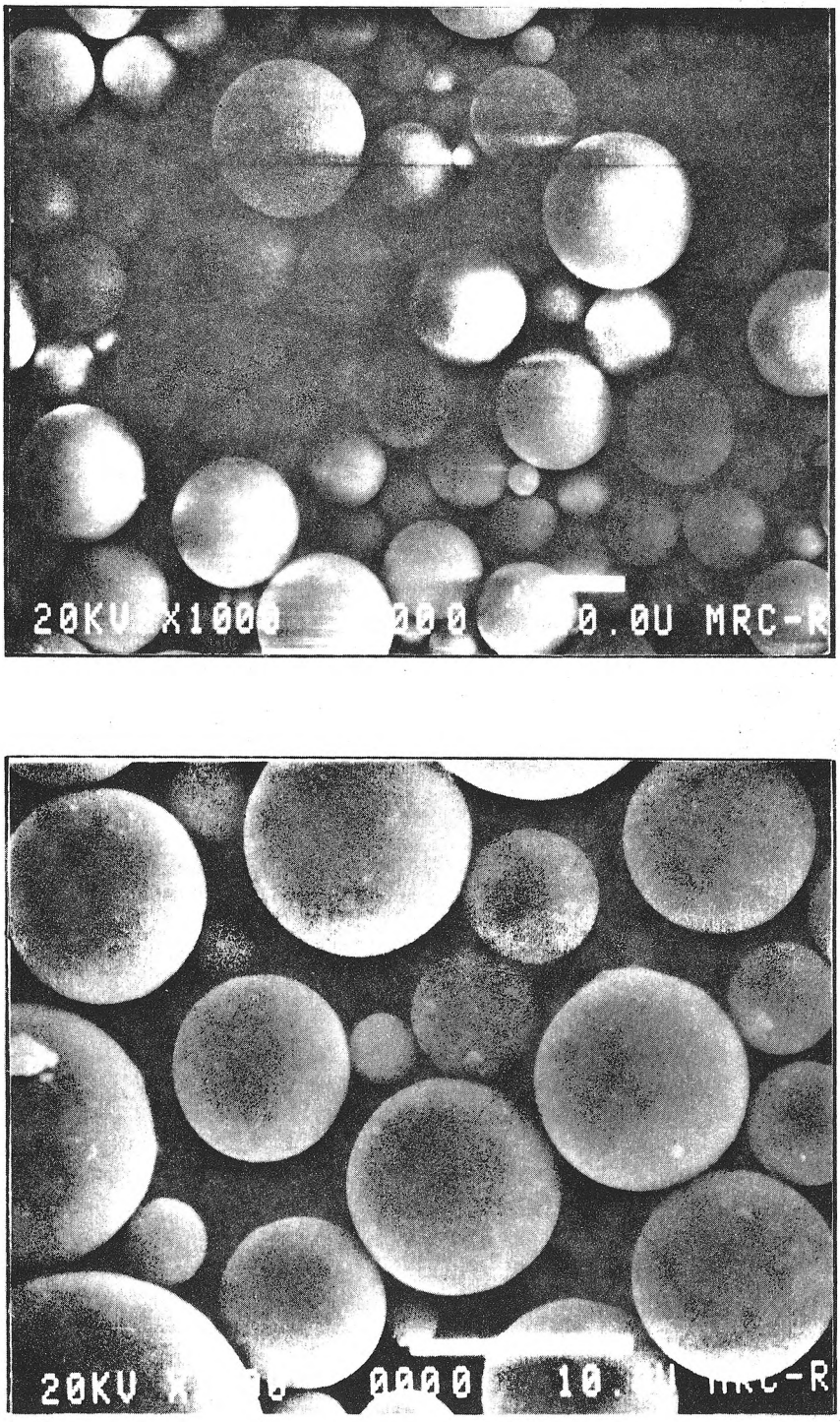

Figure 13. Microspheres Made from SmAS-41 Glass.

APPENDIX A

ACTIVATION AND PROPERTIES OF Sm-153

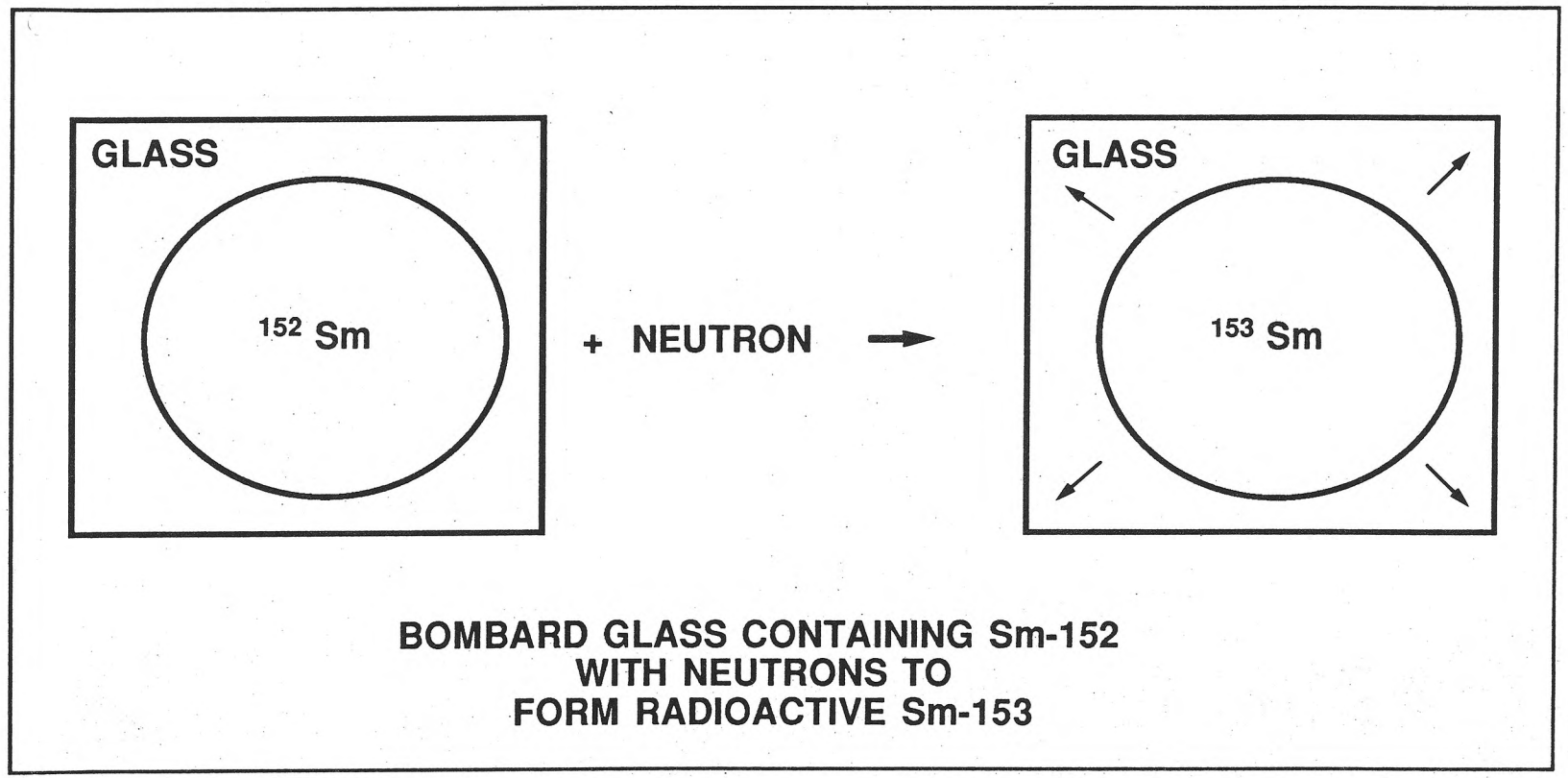

Figure 14. Activation of Sm-153.

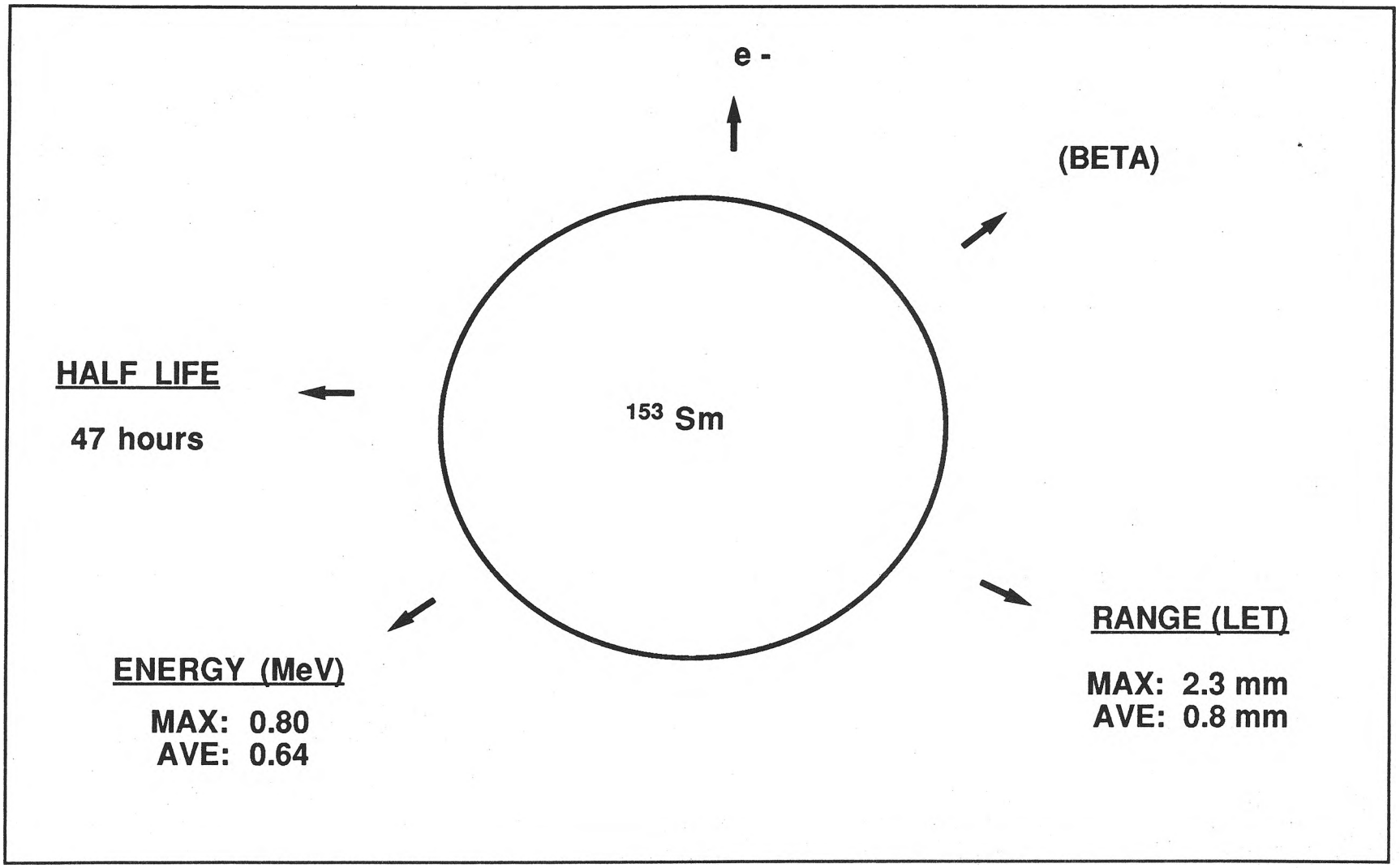

Figure 15. Properties of Sm-153.

APPENDIX B

CALCULATION OF Sm-153 ACTIVITY AND INITIAL DOSE (CURIE) AS A FUNCTION OF WEIGHT FOR $25\ Sm_2O_3 \cdot 25\ Al_2O_3 \cdot 50\ SiO_2$, MOLE %, (SmAS-33) GLASS

The decay of a radioactive material or a radionuclide is essentially random or probabilistic in nature, and, the rate of decay at any given time, depends only upon the number of active atoms present at that time. If it is assumed that after disintegration or decay the resulting daughter atom is nonradioactive, the rate of decay can be written as,

$$-\frac{dN_t}{d_t} \propto Nt \quad \ldots\ldots\ldots\ldots\ldots\ldots\ldots\ldots\ldots\ldots \quad (1)$$

Where Nt is the number of radioactive atoms present at time t. The negative sign means that the number of radioactive atom decreases after each decay. Equation (1) can be written as,

$$-\frac{dN}{d_t} = \lambda N_t \quad \ldots\ldots\ldots\ldots\ldots\ldots\ldots\ldots\ldots\ldots \quad (2)$$

Where the constant λ is a characteristic of the particular radionuclide and is known as the decay constant. Physically, λ is a measure of the probability that a particular atom will disintegrate per unit of time. Integration of Equation (2) yields,

$$\ln N_t = -\lambda_t + C \quad \ldots\ldots\ldots\ldots\ldots\ldots\ldots\ldots\ldots\ldots \quad (3)$$

where C is an integration constant. If it is assumed that at the initial time (t=0), the number of radioactive atoms present is N_0, then Equation (3) yields, $C=\ln N_0$, and

$$\ln N_t = \ln N_0 - \lambda t \quad \ldots\ldots\ldots\ldots\ldots\ldots\ldots\ldots\ldots\ldots \quad (4)$$

or,
$$\ln\left(\frac{N_t}{N_0}\right) = -\lambda t \quad \ldots\ldots\ldots\ldots\ldots\ldots\ldots\ldots\ldots\ldots \quad (5)$$

or,
$$N_t = N_0 e^{-\lambda t} \quad \ldots\ldots\ldots\ldots\ldots\ldots\ldots\ldots\ldots\ldots \quad (6)$$

The number of radioactive atoms (N) present at any time is difficult to measure, but the radiation emitted from the atom after decay is detectable, so a term "activity", A, defined as,

$$A = \frac{-dN}{d_t} = \lambda N \quad \ldots\ldots\ldots\ldots\ldots\ldots\ldots\ldots\ldots\ldots \quad (7)$$

is used to measure the radioactivity of an element at a particular time. Here, 'A' measures the number of decays per unit time at a particular instant from an assemblage of N radioactive atoms. Multiplying both sides of Equation (6) by λ, one obtains,

$$A_t = A_0 e^{-\lambda t} \quad \ldots\ldots\ldots\ldots\ldots\ldots\ldots\ldots\ldots\ldots \quad (8)$$

Where $A_t = \lambda N_t$ and $A_0 = \lambda N_0$ is the activity at time t and initial time (t=0), respectively.

The activity of a radionuclide, therefore, decays exponentially according to Equation (8) and theoretically never becomes zero. Depending upon the value of λ, different radionuclides decay at different rates.

A term, $t_{1/2}$, known as the half life, gives a physical meaning to the life of a radionuclide. The half life $t_{1/2}$, is defined as the time required for the activity to decrease to 1/2 (50%) of its original value (i.e., $\frac{A_t}{A_0} = \frac{1}{2}$)

$$\frac{A_t}{A_0} = \frac{1}{2} = e^{-\lambda t_{1/2}} \quad \ldots\ldots\ldots\ldots\ldots\ldots\ldots\ldots\ldots\ldots \quad (9)$$

$$\ln(\frac{1}{2}) = -\lambda t_{1/2} \quad \text{..... (10)}$$

or, $$\ln(2) = \lambda t_{1/2} \quad \text{..... (11)}$$

or, $$t_{1/2} = \frac{0.693}{\lambda} \quad \text{..... (12)}$$

A radionuclide with a long half life, $t_{1/2}$, means that λ will be small. For Sm-153, $t_{1/2}$ = 46.3 hours. Therefore, λ for Sm-153 = $\frac{0.693}{46.3} = 14.97 \times 10^{-3} h^{-1}$ or $4.16 \times 10^{-6}\ s^{-1}$. The time dependence for the activity of Sm-153 can be expressed, therefore, as,

$$A_t = A_0 e^{-(4.16 \times 10^{-6}\ s^{-1})t} \quad \text{..... (13)}$$

A plot of $\frac{A_t}{A_0}$ vs. time for Sm-153 Equation (13) is shown in Figure 16, which is the decay curve for Sm-153. The time required for the activity of Sm-153 to decay by 99.9%, which for all practical purposes, can be considered as the effective end of the decay process, can be calculated as,

$$t = \ln(\frac{A_0}{A_t})\frac{1}{\lambda} = \ln(\frac{100}{.1})\frac{1}{4.16 \times 10^{-6} 5^{-1}} = 1.66 \times 10^6\ s = 19.22\ \text{days} \quad \text{..... (14)}$$

To calculate the dosage and activity in a specific glass, Equation (13) must be expanded to account for specific irradiation variables and radionuclide properties. The production of Sm-153 by neutron bombardment is as follows:

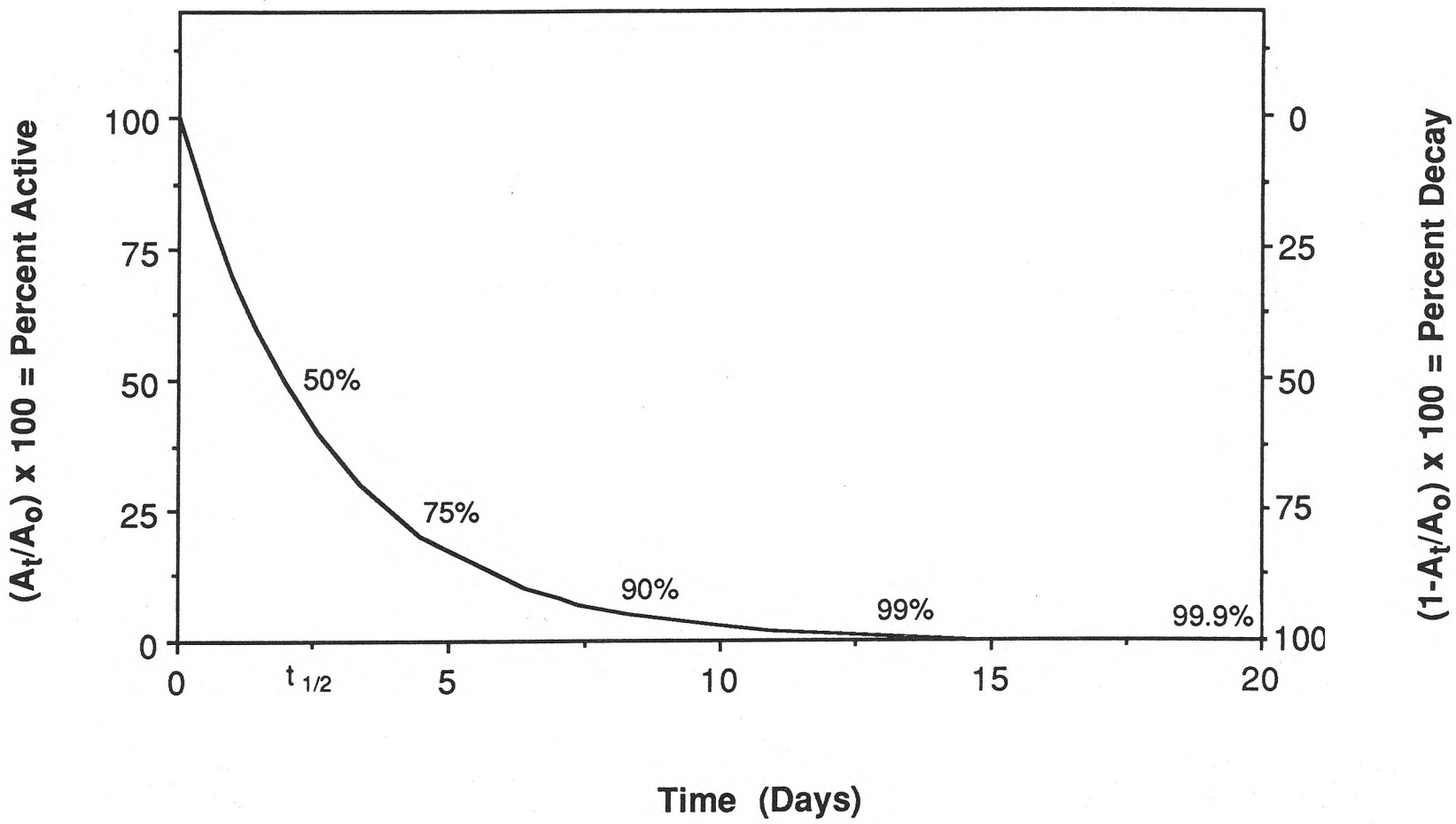

Figure 16. Decay Curve for Sm-153.

$$^{152}Sm \xrightarrow{(n,\gamma)} {}^{153}Sm \xrightarrow{\beta^-} \quad \text{..... (15)}$$

The radionuclide properties which are important to calculating the activity are the half life, (46.3 h), isotopic abundance (26.7 %), and the thermal and resonance cross-section (220 b and 3168 b, respectively). The thermal cross-section (σ_t) is for production from thermal energy neutrons (primary neutrons in the reactor). The resonance cross-section (σ_r) is for production from slightly higher energy neutrons (resonance region neutrons).

The neutron fluxes (ϕ) are characteristics of the irradiation process such that ϕ_t (thermal) >> ϕ_r (resonance). The general equation is

$$A = N \sigma \phi (1 - e^{-\lambda t})(e^{-\lambda T}) \quad \text{..... (16)}$$

where A = activity (mCi)

N = number of target atoms

ϕ = neutron flux

σ = neutron cross-section (reaction probability)

t = irradiation time

T = decay time after irradiation

λ = decay constant

The term $(1 - e^{-\lambda t})$ is called the saturation factor and will approach 1.0 for irradiation times much larger than the half life ($t_{1/2}$). The term $(e^{-\lambda T})$ is called the decay factor after irradiation.

In general, the overall activity curve can be seen in Fig. 17. The activity builds up until it is decaying as rapidly as it is being produced, at which point (saturation) it remains constant until the sample is removed from the reactor; then the sample begins to decay. At no time are all of the Sm-152 nuclei used up (i.e., saturation does not mean that all of the possible

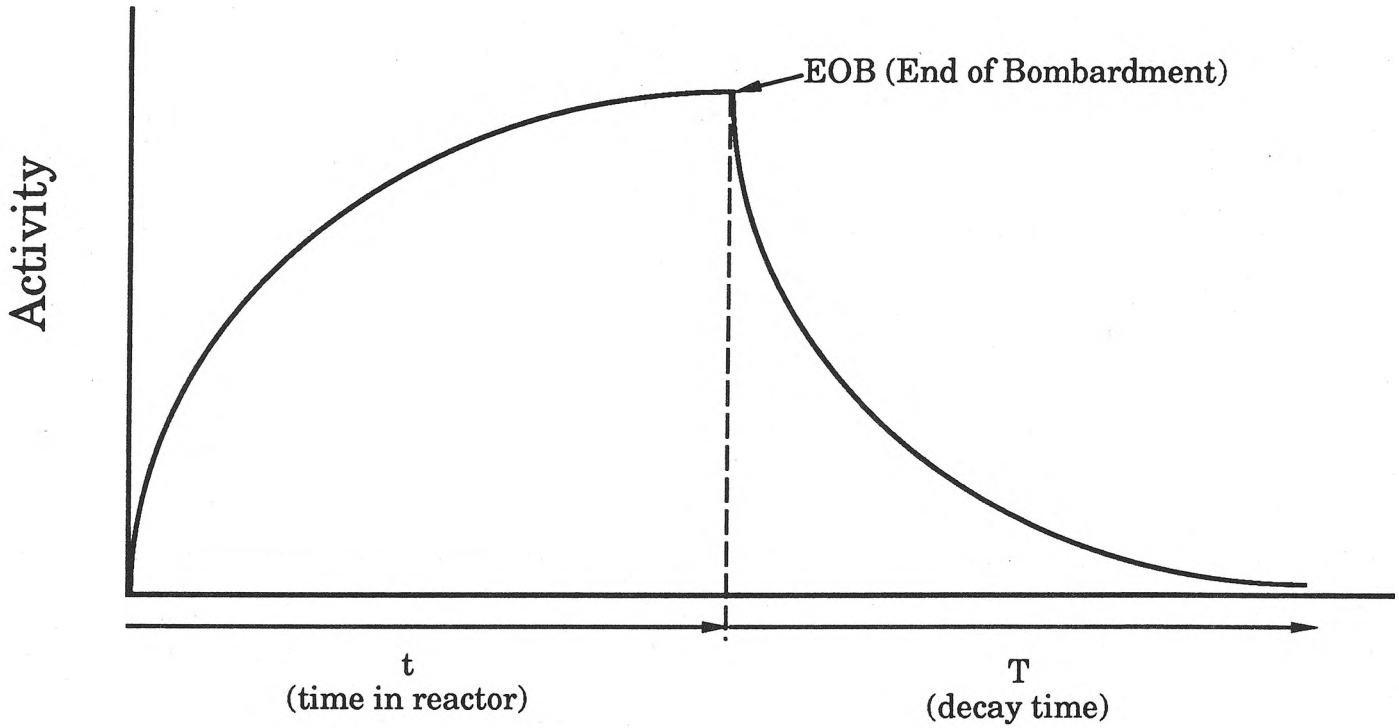

Figure 17. Overall Activity Curve for a Radionuclide.

captures have occurred). In general , only a small fraction (<1 %) of Sm-152 will have undergone neutron capture.

Consider 1 g of SmAS-33 irradiated for 48 h at $\phi_t = 8.0 \times 10^{13}$ and $\phi_r = 2.5 \times 10^{12}$ neutrons/cm^2·s and allowed to decay for 24 h.

GLASS COMPOSITION (SmAS-33)	MOLE %	WEIGHT %
Sm_2O_3	25	61.1
Al_2O_3	25	17.9
SiO_2	50	21.0

$$Sm_2Al_2Si_2O_{10} \rightarrow \text{(2) moles Sm} \quad \text{..... (17)}$$

$$\frac{.61\text{g } Sm_2O_3}{1\text{ g glass}} \cdot \frac{1\text{ mol } Sm_2O_3}{348.78\text{ g } Sm_2O_3} \cdot \frac{2\text{ mol Sm}}{1\text{ mol } Sm_2O_3} \cdot \frac{150.4\text{ g Sm}}{1\text{ mol Sm}} \cdot \frac{6.02 \times 10^{23}\text{ Sm-atom}}{150.4\text{g Sm}}$$

$$\rightarrow \quad 2.108 \times 10^{21} \frac{\text{Sm-atom}}{\text{g glass}} \cdot \text{(isotopic abundance = .267)} \quad \text{..... (18)}$$

$$\rightarrow \quad 5.63 \times 10^{20} \text{ Sm-atoms/g glass}$$

using Equation (16) to calculate the initial dose per mg of SmAS-33 glass,

$$A_{Sm\text{-}153} = (8.47 \times 10^{22})(6.897 \times 10^{-16}\text{ mCi})(.5128)(.698) \quad \text{..... (19)}$$

$$A_{Sm\text{-}153} = 139.05\text{ mCi/mg glass} \quad \text{..... (20)}$$

It can be seen from this calculation that several variables in the activation process can be altered to yield various initial activities.

The determination of the number of 30 μm glass microspheres per gram of glass (SmAS-33) gives understanding to the dosage received. Knowing the diameter of each microsphere and the density (4.6 g/cm^3), the number of microspheres per gram of glass can be calculated.

$\rho = 4.6\ g/cm^3 = 4.6 \times 10^{-12}\ g/\mu m^3$ ..... (21)

$V = 4/3\ \pi\ r^3 = 1.41 \times 10^4\ \mu m^3$ ..... (22)

(30μm spheres) Mass = 6.503×10^{-8} g ..... (23)

Mass = Density x Volume ..... (24)

$$\frac{1\ mg\ (Smas\text{-}33)}{6.50 \times 10^{-5}\ g} = 15.4 \times 10^3\ \frac{(30\ \mu m\ spheres)}{mg\ SmAS\text{-}33} \quad \text{..... (25)}$$

For convenience, a calibration curve (Fig. 18) is given showing the initial dose that can be obtained from the previously described activation process for a given weight of SmAS-33 glass and the number of 30 μm spheres.

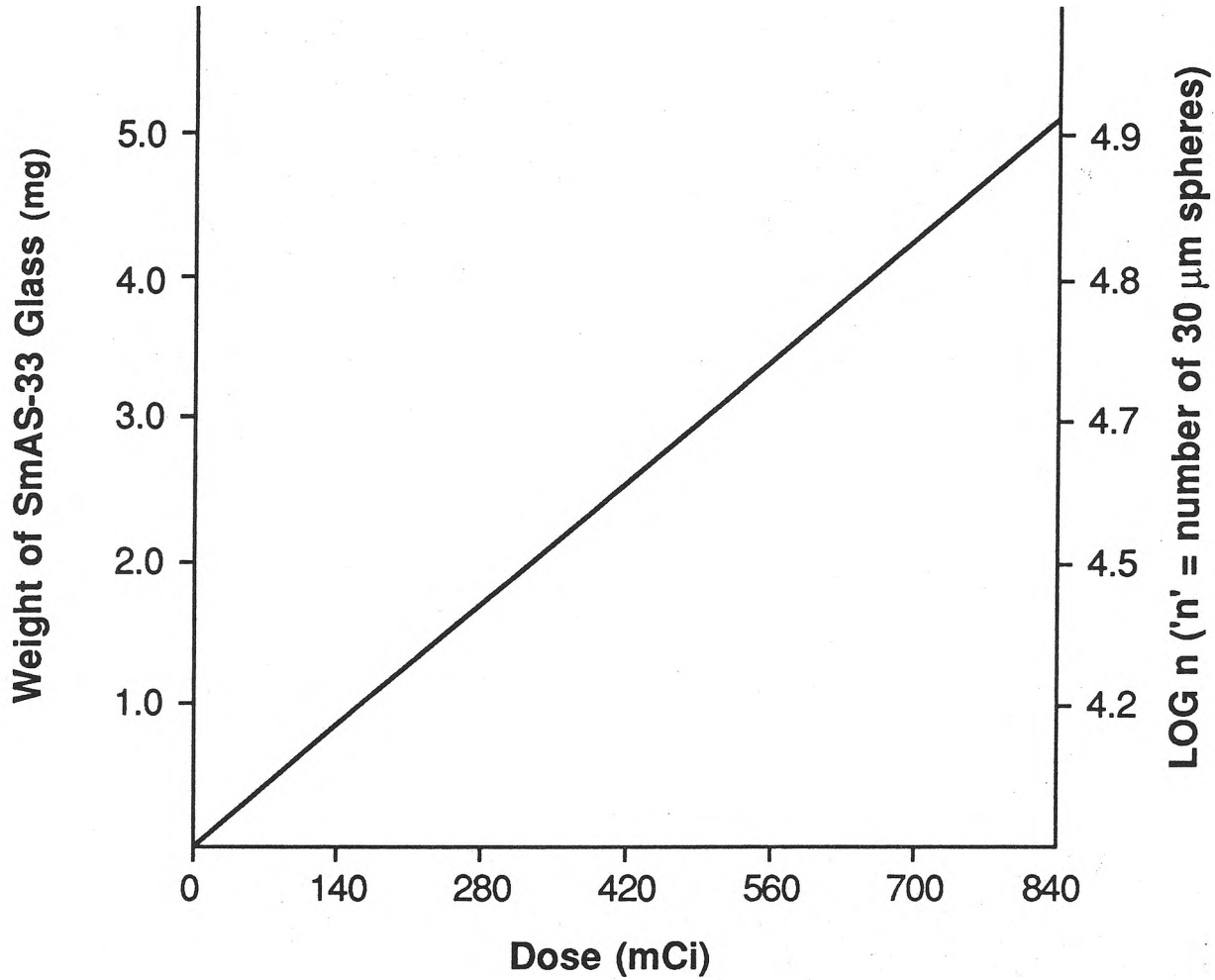

Figure 18. Calibration Curve Showing Dose as a Function of the Weight (g) of SmAS-33 Glass and the Number of Microspheres.

Summary of Calculations

1. Irradiation of 1 mg of SmAS-33 glass following the previous calculation gives an initial dose after 24 h decay, of ≈ 140 mCi and contains 15 x 10^3 microspheres 30 μm in diameter.
2. Approximately 19 d are required for complete decay (more accurately 99.99%) of Sm-153 activity.
3. If a patient is injected with 1 mg of SmAS glass, after 24 h decay, the dose remaining in the body after 46.3 hours ($t_{1/2}$) is ≈ 70 mCi and after 19 d will be 1.40 x 10^{-2} mCi.

APPENDIX C

SCHEMATIC OF SYSTEM USED TO SPHEROIDIZE GLASS POWDER

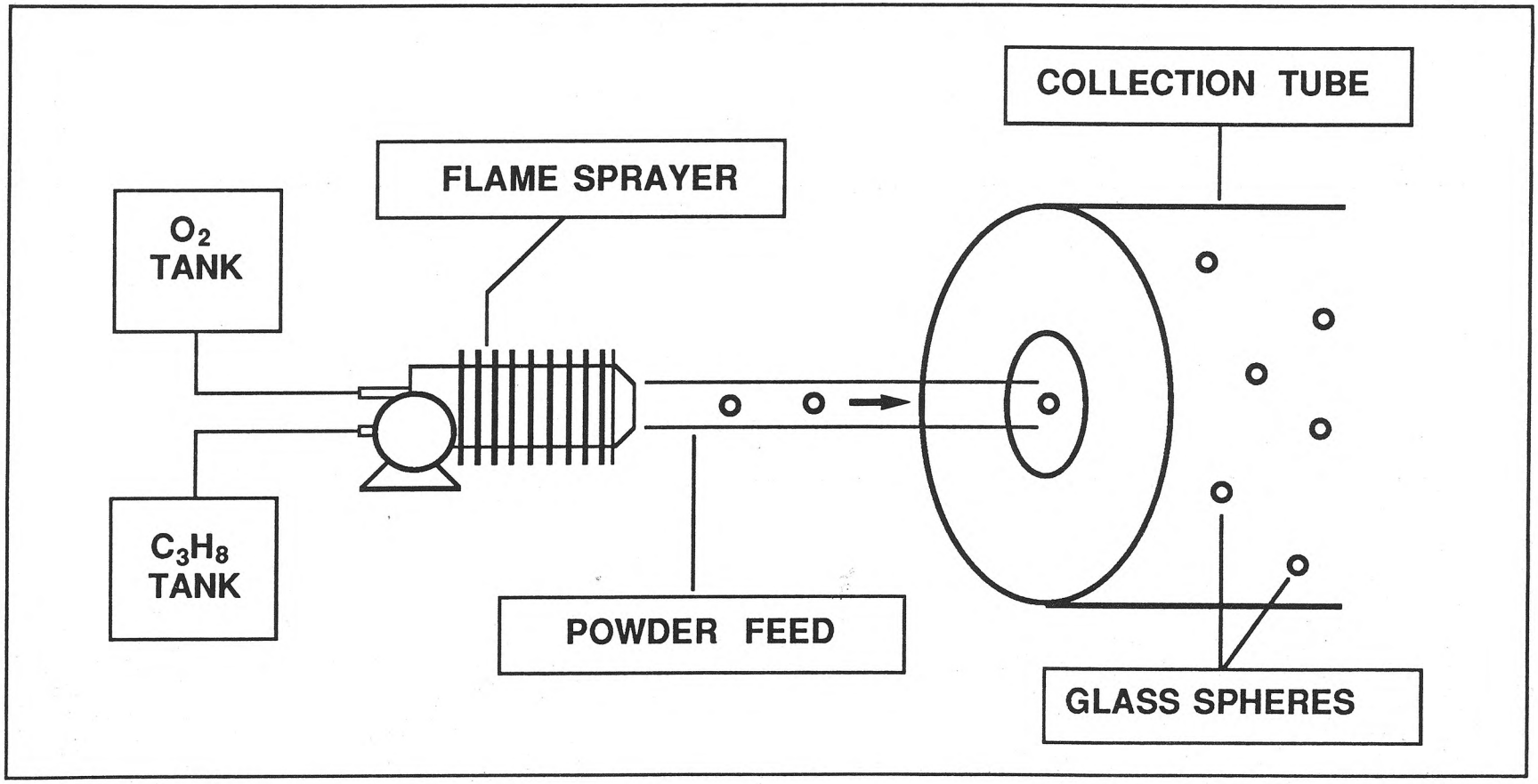

Figure 19. Schematic of System Used to Spheroidize Glass Powder.